

# Journal Pre-proof

Tariquidar-related triazoles as potent, selective and stable inhibitors of ABCG2 (BCRP)

Frauke Antoni, Manuel Bause, Matthias Scholler, Stefanie Bauer, Simone A. Stark, Scott M. Jackson, Ioannis Manolaridis, Kaspar P. Locher, Burkhard König, Armin Buschauer, Günther Bernhardt

PII: S0223-5234(20)30100-8

DOI: <https://doi.org/10.1016/j.ejmech.2020.112133>

Reference: EJMECH 112133

To appear in: *European Journal of Medicinal Chemistry*

Received Date: 31 October 2019

Revised Date: 4 February 2020

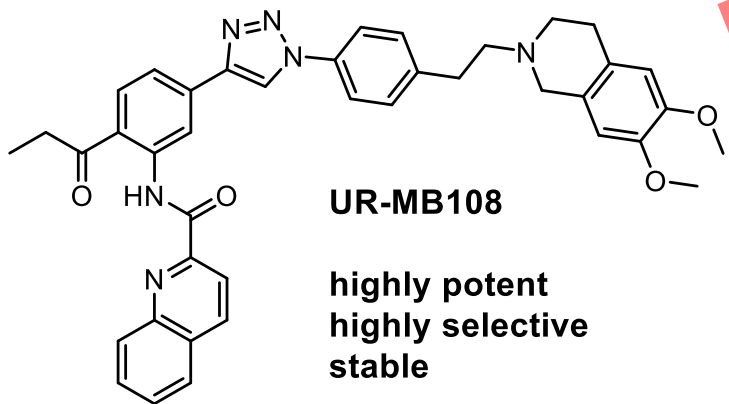
Accepted Date: 6 February 2020

Please cite this article as: F. Antoni, M. Bause, M. Scholler, S. Bauer, S.A. Stark, S.M. Jackson, I. Manolaridis, K.P. Locher, B. König, A. Buschauer, G. Bernhardt, Tariquidar-related triazoles as potent, selective and stable inhibitors of ABCG2 (BCRP), *European Journal of Medicinal Chemistry* (2020), doi: <https://doi.org/10.1016/j.ejmech.2020.112133>.

This is a PDF file of an article that has undergone enhancements after acceptance, such as the addition of a cover page and metadata, and formatting for readability, but it is not yet the definitive version of record. This version will undergo additional copyediting, typesetting and review before it is published in its final form, but we are providing this version to give early visibility of the article. Please note that, during the production process, errors may be discovered which could affect the content, and all legal disclaimers that apply to the journal pertain.

© 2020 Published by Elsevier Masson SAS.



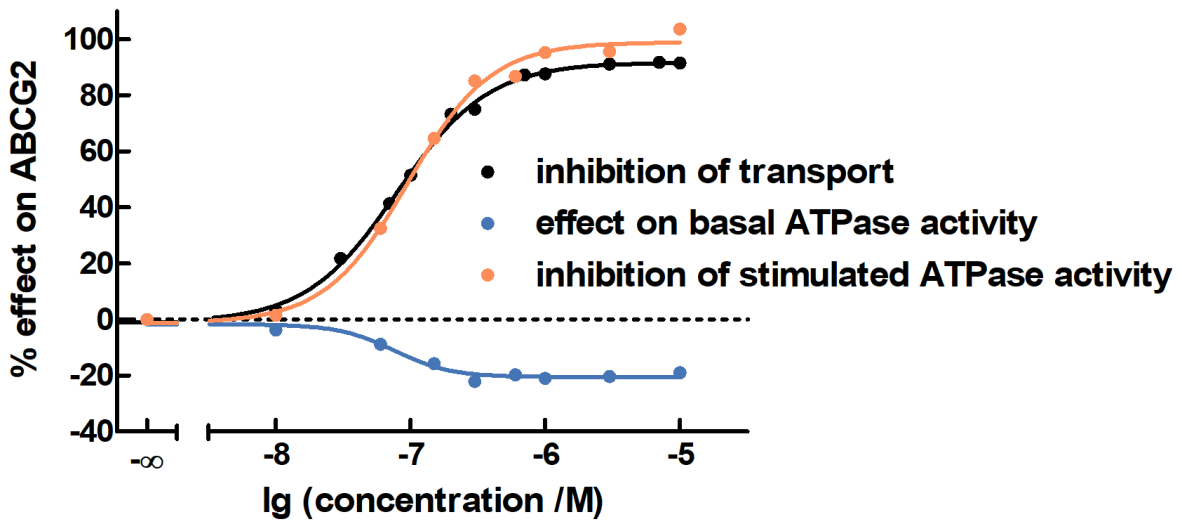
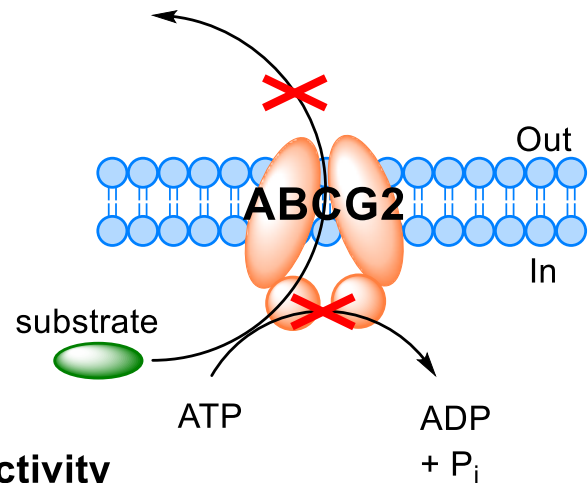


**inhibition**

**inhibition**

transport activity

ATPase activity



# Tariquidar-Related Triazoles as Potent, Selective and Stable Inhibitors of ABCG2 (BCRP)

Frauke Antoni<sup>a,\*</sup>, Manuel Bause<sup>b</sup>, Matthias Scholler<sup>a</sup>, Stefanie Bauer<sup>a</sup>, Simone A. Stark<sup>b</sup>, Scott M. Jackson<sup>c</sup>, Ioannis Manolaridis<sup>c</sup>, Kaspar P. Locher<sup>c</sup>, Burkhard König<sup>b,\*</sup>, Armin Buschauer<sup>a,#</sup>, Günther Bernhardt<sup>a</sup>

<sup>a</sup> *Institute of Pharmacy, University of Regensburg, D-93040 Regensburg, Germany*

<sup>b</sup> *Institute of Organic Chemistry, University of Regensburg, D-93040 Regensburg, Germany*

<sup>c</sup> *Institute of Molecular Biology and Biophysics, ETH Zürich, CH-8093 Zürich, Switzerland*

## Abstract

Tariquidar derivatives have been described as potent and selective ABCG2 inhibitors. However, their susceptibility to hydrolysis limits their applicability. The current study comprises the synthesis and characterization of novel tariquidar-related inhibitors, obtained by bioisosteric replacement of the labile moieties in our previous tariquidar analog UR-ME22-1 (**9**). CuAAC (“click” reaction) gave convenient access to a triazole core as a substitute for the labile amide group and the labile ester moiety was replaced by different acyl groups in a Sugasawa reaction. A stability assay proved the enhancement of the stability in blood plasma. Compounds UR-MB108 (**57**) and UR-MB136 (**59**) inhibited ABCG2 in a Hoechst 33342 transport assay with an IC<sub>50</sub> value of about 80 nM and belong to the most potent ABCG2 inhibitors described so far. Compound **57** was highly selective, whereas its PEGylated analog **59** showed some activity at ABCB1. Both **57** and **59** produced an ABCG2 ATPase-depressing effect which is in agreement with our precedent cryo-EM study identifying **59** as an ATPase inhibitor that exerts its effect via locking the inward-facing conformation. Thermostabilization of ABCG2 by **57** and **59** can be taken as a hint to comparable binding to ABCG2. As reference substances, compounds **57** and **59** allow additional mechanistic studies on ABCG2 inhibition. Due to their stability in blood plasma, they are also applicable in vivo. The highly specific inhibitor **57** is suited for PET labeling, helping to further elucidate the (patho)physiological role of ABCG2, e.g. at the BBB.

## Keywords

ABCG2 transporter, BCRP, inhibitors, multidrug resistance, Hoechst33342, ATPase

# 1 Introduction

In 1990, a novel drug resistance-related membrane protein was discovered in a doxorubicin resistant breast cancer cell line [1] and in 1998 it was identified as the most recent member of the human ABC transporter superfamily and named breast cancer resistance protein (BCRP) [2]. The Human Genome Nomenclature Committee termed the transporter ABCG2 [3]. ABCG2 as well as other ABC transporter subtypes such as ABCB1 (P-gp) and ABCC1 (MRP1) are not only associated with the chemoresistance of malignant tumors [4-7], but they are also expressed at the blood-brain barrier (BBB), preventing the entry of a broad variety of xenobiotics, including numerous drugs, into the central nervous system [8-10]. Therefore, co-administration of an ABC inhibitor and a cytostatic drug represents an attractive strategy to overcome the BBB and multidrug resistance (MDR) of various malignancies. This has been demonstrated by several proof-of-concept studies, although ABC inhibitors are not in clinical use yet [11-16]. ABCG2 has come into focus since apart from being one of the three major subtypes conferring MDR in cancer cells (in addition to ABCB1 and ABCC1), it also appears to be the most abundant subtype at the human BBB [17, 18].

Figure 1 shows a selection of ABCG2 inhibitors described so far. Among the first substances found to affect ABCG2 activity are inhibitors of the ABCB1 transporter, primarily the benzanilides elacridar (**1**) and tariquidar (**2**) [19-22]. Fumitremorgin C (FTC) (**3**), a fungal toxin from *A. fumigatus* Fresen. containing a tetrahydro- $\beta$ -carboline backbone, was the first known specific inhibitor of the ABCG2 subtype [23]. Its neurotoxic effects, however, preclude its use in vivo. Its nontoxic analog Ko143 (**4**) was developed in 2002 and is still among the most potent known ABCG2 inhibitors [24]. It was recently reported, though, that it also interferes with both, ABCB1 and ABCC1 transport, but only at higher concentrations (low micromolar range) [25]. The suitability of Ko143 for in vivo studies is compromised by the poor metabolic stability of the ester moiety [26, 27]. Lately, further derivatives of FTC have been produced, e.g. compound **5** [28]. Besides the fungal toxin FTC, other natural compounds and derivatives thereof were reported to antagonize ABCG2, the main structural class being flavonoids such as flavones, chalcones and curcuminoids [29-34]. Chromone is a partial structure present in many active flavonoids and was derivatized to create novel, potent and nontoxic ABCG2 inhibitors such as compounds **6** and **7** [35]. The stability of these compounds still remains to be determined, though. In an ongoing search for potent, selective and stable inhibitors for ABCG2, further structure types have emerged, for instance the relatively small acrylonitrile YHO-13177 (**8**) [36, 37].

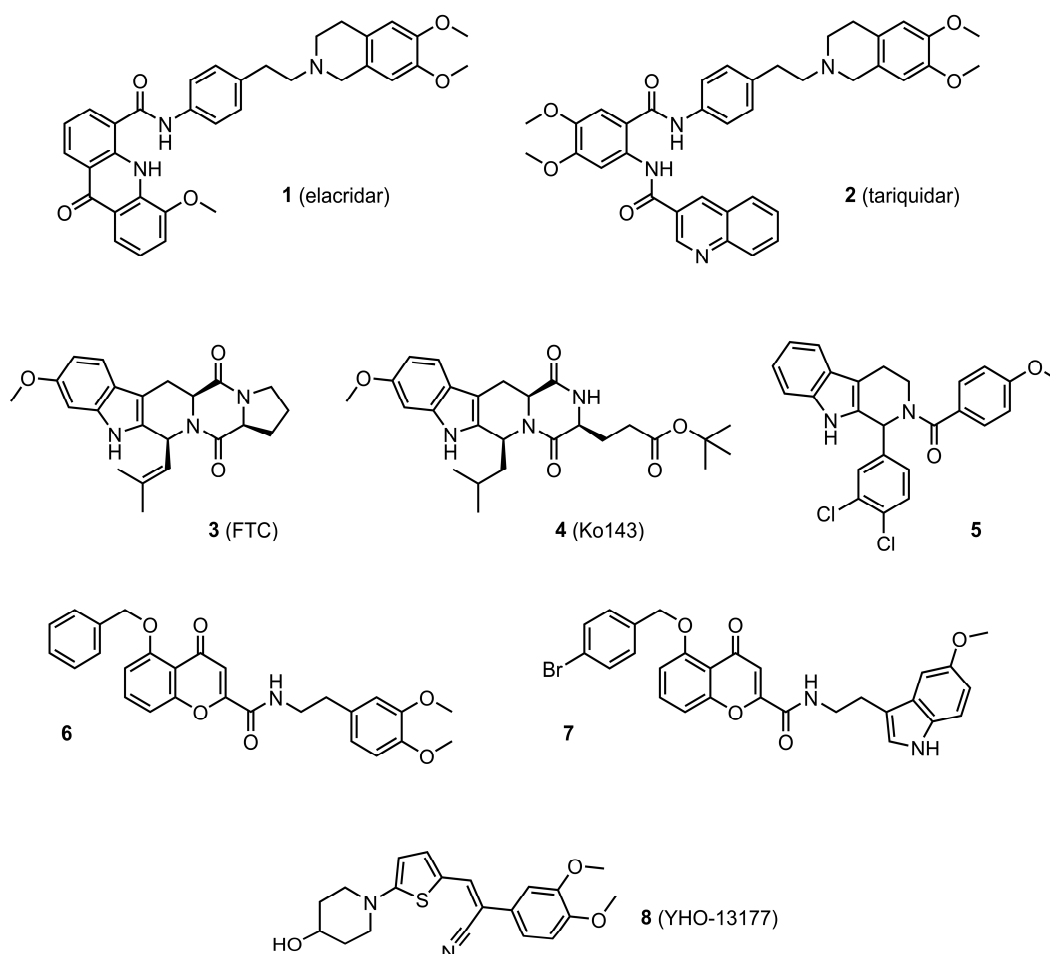


**Figure 1.** Structures of known ABCG2 inhibitors: elacridar (**1**), tariquidar (**2**), fumitremorgin C (**3**), Ko143 (**4**), the  $\beta$ -carboline derivative **5**, the chromones **6** and **7** and the acrylonitrile YHO-13177 (**8**).

Until recently, the mechanism of ABCG2 inhibition could only be speculated about, since there were no high-resolution structural data for ABCG2. The breakthrough came in 2017 with the high-resolution cryo-EM structure of ABCG2 [38]. One year later, we determined the structure of ABCG2 in complex with two different inhibitors, including UR-MB136 (**59**), a member of the series we present here [39]. The synthetic route to **59**, the appertaining series of novel ABCG2 inhibitors and their biological characterization have not been published yet, and are subject of the present study. Heretofore, we modified the dual ABCB1/ABCG2 inhibitor tariquidar (**2**) to obtain the selective ABCG2 inhibitor UR-ME22-1 (**9**) (Figure 2) [40]. The main, selectivity-yielding modification was the shift of the hetarycarboxamido moiety from the *ortho*- to the *meta*-position of the central benzamide core. However, this shift rendered the central benzamide bond prone to hydrolysis in murine plasma, presumably due to inadequate steric hindrance, facilitating the attack of the amide bond by plasma esterases. In an attempt to gain stable tariquidar analogs, the labile amide moiety was replaced by an indole ring, yielding more stable inhibitors with higher efficacy than **9** [41]. However, it was shown that these compounds were still hydrolysed to a certain extent, namely at the ester

bond attached to the central, trisubstituted phenyl ring. Here we present the synthesis and pharmacological evaluation of novel tariquidar derivatives. As shown in Figure 2, we introduced a triazole core as a bioisoster to the labile amide group in **9**, which can be more conveniently synthesized than an indole moiety. Furthermore, we synthesized compounds in which the labile ester moiety was replaced by ketone groups. We aimed at ABCG2 inhibitors that are potent, effective, selective, and suitable for complexing with ABCG2 in cryo-EM experiments and, moreover, also stable in blood plasma, a prerequisite for in vivo studies.

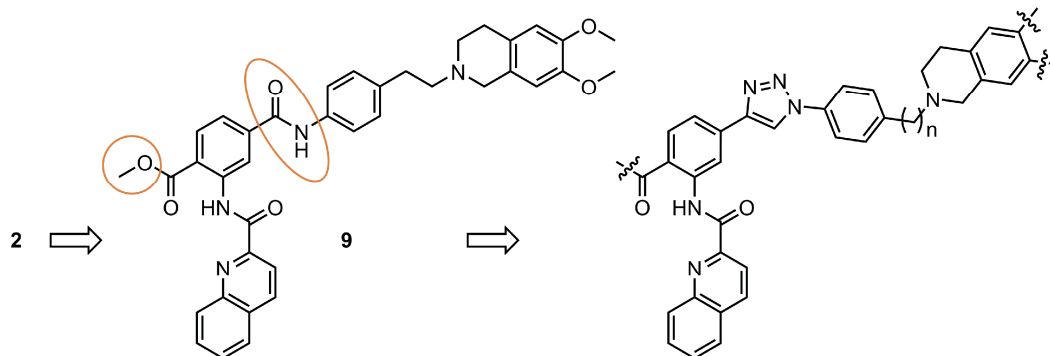


**Figure 2.** Structure of UR-ME22-1 (**9**) and general structures of the title compounds developed from **9**.

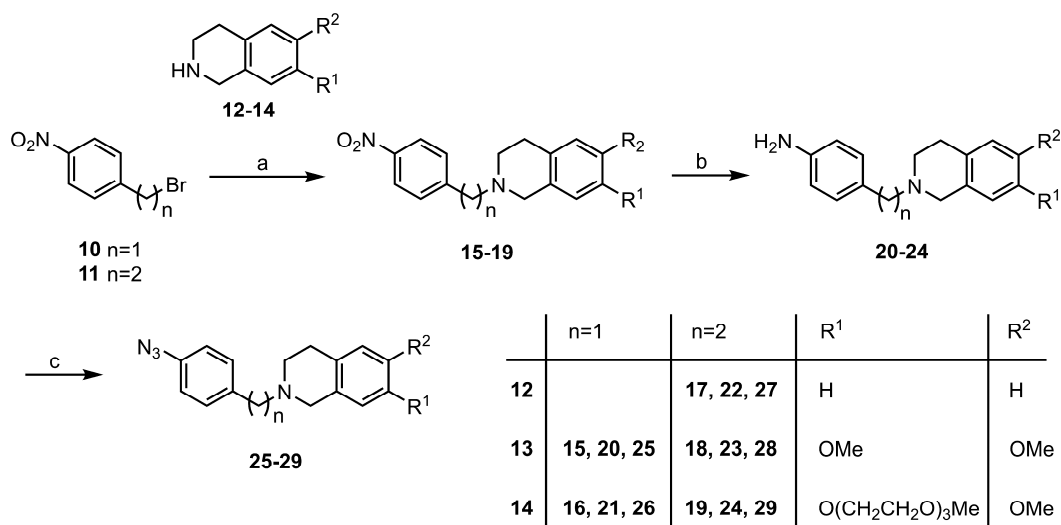
In order to rank our novel series we also purchased or prepared compounds **2-8** as reference substances and investigated them in our assays.

## 2 Results and Discussion

### 2.1 Synthesis

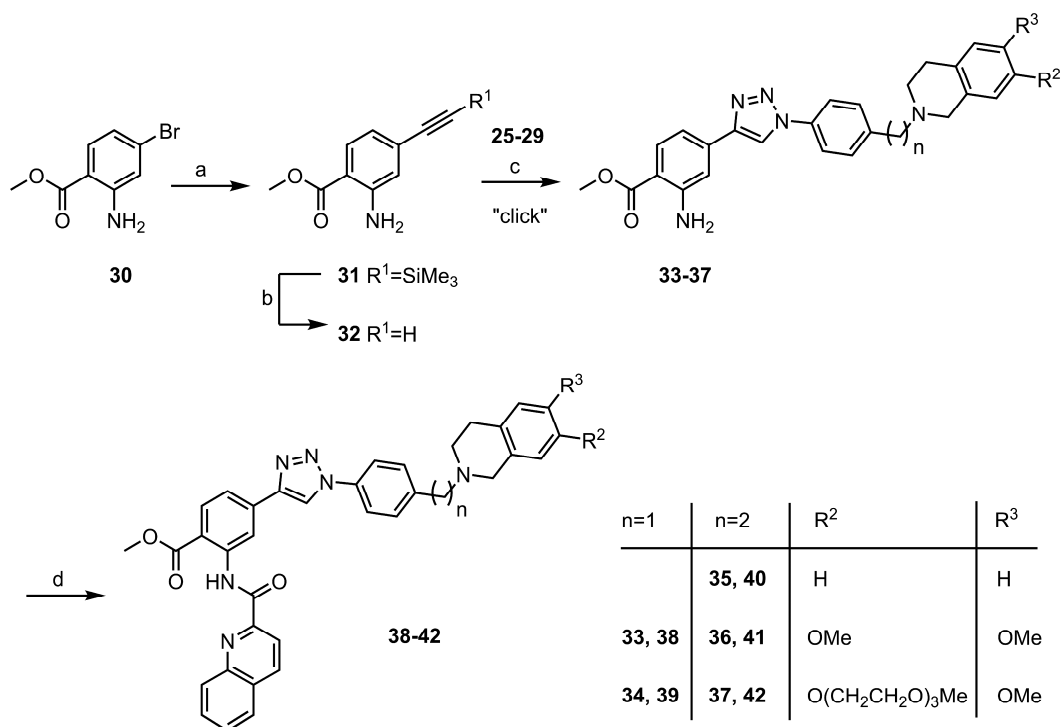
“Key” step in the convergent synthesis of the title compounds was the production of the triazole core in a copper-catalyzed azide-alkyne cycloaddition (CuAAC), a stepwise variant of the Huisgen cycloaddition process, and the most often used “click” reaction [42]. Here we used the polytriazole TBTA as a copper(I)-stabilizing ligand [43]. The azides for the CuAAC were prepared in three steps (Scheme 1). In order to vary the linker length between the tetrahydroisoquinoline moiety and the phenyl ring, either 1-(bromomethyl)-4-nitrobenzene (**10**) or 1-(2-bromoethyl)-4-nitrobenzene (**11**) was combined with the respective tetrahydroisoquinoline derivative (**12-14**) in an *N*-alkylation reaction affording compounds **15-19**. In our previous studies on tariquidar analogs it proved to be advantageous in terms of efficacy to introduce a polyethylene glycol (PEG) chain at the tetrahydroisoquinoline moiety, which was explained by a solubilizing effect [41, 44, 45]. For this reason, we also synthesized the PEGylated tetrahydroisoquinoline derivative **14** according to our previous report [44] and alkylated the nitrogen. In the next two steps, the nitro group in compounds **15-19** was reduced

to an amine group, resulting in compounds **20-24**, and then converted into an azide moiety, affording compounds **25-29**.



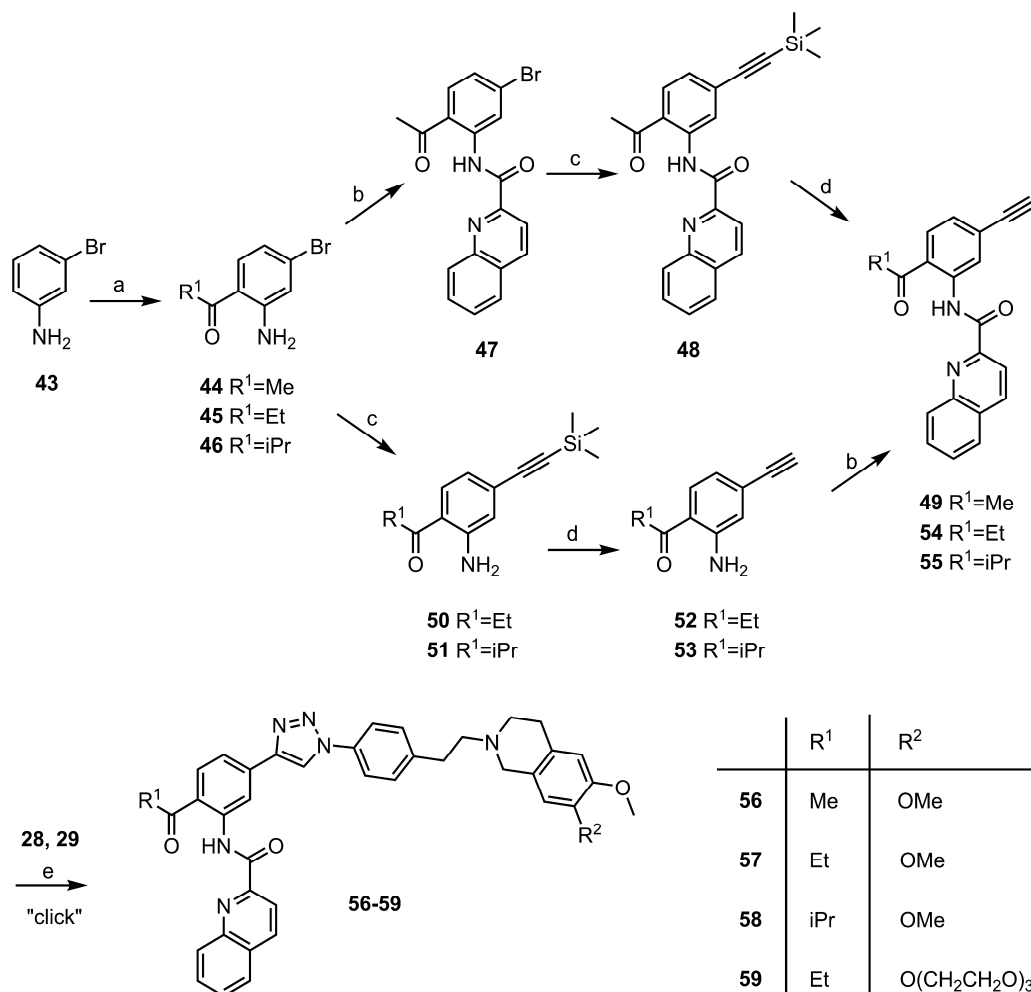
**Scheme 1.** Synthesis of the azides for the “click” reactions. Reagents and conditions: (a) K<sub>2</sub>CO<sub>3</sub>, MeCN, reflux, overnight; (b) Pd/C, H<sub>2</sub> (40 bar), EtOH, rt, overnight or SnCl<sub>2</sub>, EtOH, reflux, 2 h; (c) (I) NaNO<sub>2</sub>, 6 M HCl aq, -5 °C, 1 h; (II) NaN<sub>3</sub>, -5 °C, 1 h.

The synthesis of the target compounds containing an ester group is shown in Scheme 2. Firstly, the alkyne (**32**) as the second reactant in the “click” reactions was prepared by Sonogashira coupling of methyl 2-amino-4-bromobenzoate (**30**) and trimethylsilylacetylene to **31** and subsequent TMS-deprotection to compound **32**. Then **32** was combined with the azides **25-29**, affording the triazoles **33-37** and the quinoline moiety was introduced by amide coupling with quinoline-2-carboxylic acid, yielding the inhibitors **38-42**.



**Scheme 2.** Synthesis of the inhibitors **38-42** bearing an ester moiety. Reagents and conditions: (a) ethynyltrimethylsilane, Pd(PPh<sub>3</sub>)<sub>2</sub>Cl<sub>2</sub>, CuI, NEt<sub>3</sub>, THF, 60 °C, overnight; (b) TBAF, THF, 0 °C, 2 h; (c) CuSO<sub>4</sub>, sodium ascorbate, TBTA, DMF, rt, 24 h; (d) quinoline-2-carboxylic acid, HBTU, DIPEA, DCM, 0 °C → rt, 24 h.

In the second subseries, the labile ester moiety was replaced by different ketone groups (Scheme 3). 3-Bromoaniline (**43**) was acylated in a Sugasawa reaction, a specific *ortho*-acylation of anilines, to form the ketones **44-46**. Compound **44** was first treated with quinoline-2-carboxylic acid to form the amide **47** and then submitted to a Sonogashira coupling with trimethylsilylacetylene (resulting in **48**) and deprotected to **49**. Precursors **45** and **46** were first coupled with trimethylsilylacetylene under Sonogashira conditions (forming **50** and **51**), deprotected (to **52** and **53**), and then treated with quinoline-2-carboxylic acid to form the amide bond (yielding **54** and **55**). The final step was the “click” reaction of the alkynes **49**, **54**, and **55** with the azides **28** or **29** to form the inhibitors **56-59**.



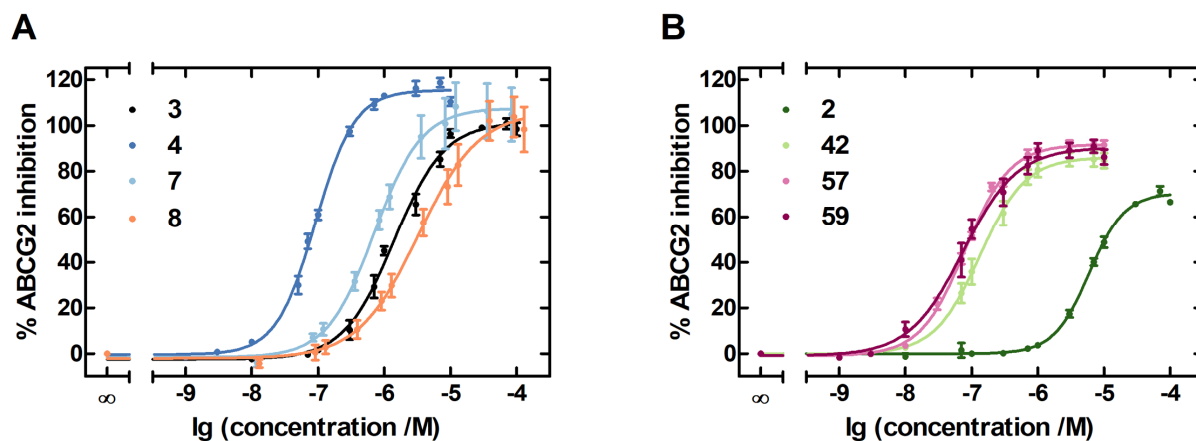
**Scheme 3.** Synthesis of the inhibitors **56-59** bearing a ketone moiety. Reagents and conditions: (a) (I)  $\text{BCl}_3$ , DCM,  $0^\circ\text{C}$ , 20 min; (II)  $\text{AlCl}_3$ , respective nitrile, reflux, 24 h; (III) 2 M HCl aq,  $0^\circ\text{C}$ , 10 min  $\rightarrow$   $80^\circ\text{C}$ , 1 h; (b) quinoline-2-carboxylic acid, HBTU, DIPEA, DCM,  $0^\circ\text{C} \rightarrow \text{rt}$ , 24 h; (c) ethynyltrimethylsilane,  $\text{Pd}(\text{PPh}_3)_2\text{Cl}_2$ , CuI,  $\text{NEt}_3$ , THF,  $60^\circ\text{C}$ , overnight; (d) TBAF, THF,  $0^\circ\text{C}$ , 2 h; (e)  $\text{CuSO}_4$ , sodium ascorbate, TBTA, DMF or THF, rt, 24 h.

The reference compounds **3** and **4** were commercially available; **2** [21], **5** [28], **6** [35], **7** [35], and **8** [36, 37] were synthesized according to literature.

## 2.2 Inhibition of the ABCG2, ABCB1 and ABCC1 Transporter Function

The newly synthesized compounds (**38-42** and **56-59**), as well as our previous tariquidar analog **9** and the reference compounds **2-8**, were analyzed for inhibition of the ABCG2 transport activity in the Hoechst 33342 microplate assay. The DNA stain Hoechst 33342, which emits blue fluorescence when bound to DNA, is a substrate of the ABCG2 transporter and therefore extruded from ABCG2-expressing cells such as the MCF-7/Topo cells utilized in this assay. When the ABCG2 transport function is inhibited, Hoechst 33342 accumulates in the cells and can be detected fluorometrically, which allows for determination of the inhibitory potency and efficacy of the target compounds. Examples of concentration-response curves are shown in Figure 3. In order to assess the selectivity of the inhibitors, they were also analyzed in the calcein-AM microplate assays with respect to inhibition of the ABCB1 and

ABCC1 transporter activity, using KB-V1 and MDCK.2-MRP1 cells, respectively. The assay principle is analogous to the Hoechst 33342 assay. The dual ABCB1 and ABCC1 substrate calcein-AM is added to the cells and exported by the respective transporter. Upon inhibition of the transport, calcein-AM accumulates in the cells, becomes cleaved to calcein by intracellular esterases and complexes  $\text{Ca}^{2+}$ -ions, resulting in a strong green fluorescence. The fluorescence can be detected and correlated with the inhibitory potencies of the test compounds. The results of the transport assays are summarized in Table 1.

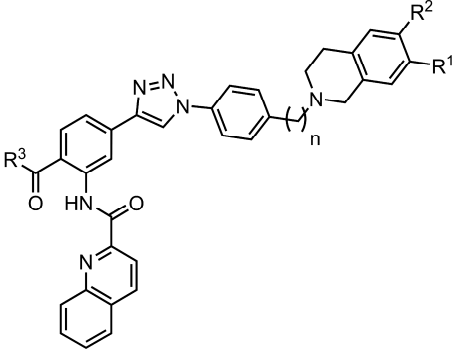


**Figure 3.** Concentration-dependent inhibition of ABCG2-mediated Hoechst efflux in MCF-7/Topo cells by (A) the reference compounds FTC (**3**), Ko143 (**4**), **7** and **8** as well as (B) tariquidar (**2**) and its novel analogs **42**, **57** and **59**. The inhibition is expressed relative to the maximal effect in the presence of 10  $\mu\text{M}$  FTC set to 100%.

FTC (**3**), its well-known analog Ko143 (**4**) and the more recent analog **5**, which all comprise a tetrahydro- $\beta$ -carboline moiety, were similarly effective at ABCG2 with an  $I_{\text{max}}$  value of 102%, 116% and 111%, respectively. However **4**, with an  $\text{IC}_{50}$  value of 92 nM, was over ten times more potent than the other two tetrahydro- $\beta$ -carboline derivatives in our assay. Whereas **4** is reported to be more potent than its precursor **3** [24], the  $\text{IC}_{50}$  value of **5** determined here (1.1  $\mu\text{M}$ ) was about five times higher than reported in literature (lit. 233 nM in Hoechst 33342 assay [28]; 237 nM in pheophorbide A assay [28]). This discrepancy probably reflects differences in the assay set-up, for instance different concentrations of Hoechst 33342 were applied (it was higher in our assay). In accordance with previous reports [25], **4** was not entirely selective; in contrast to **3** and **5** it showed activity at the ABCB1 and ABCC1 transporter. The reference compounds **6-8** were almost equieffective with **4**, but less potent. The chromone **7** inhibited ABCG2 with an  $\text{IC}_{50}$  value of 707 nM (lit. 110 nM [35]), being almost three times more potent than the chromone **6**, which showed an  $\text{IC}_{50}$  value of 1.8  $\mu\text{M}$  (lit. 170 nM [35]). Here again, the  $\text{IC}_{50}$  values determined by us were higher than those reported in literature. Furthermore, chromone **7**, as opposed to chromone **6**, showed very low inhibition of ABCB1 and ABCC1. The acrylonitrile **8** inhibited ABCG2 with a far higher  $\text{IC}_{50}$  value (3.3  $\mu\text{M}$ ) than **4**. This compound is interesting insofar as it appears to be a triple

ABCG2, ABCB1 and ABCC1 inhibitor, which might have a different application than specific inhibitors.

In accordance with previous publications [22], tariquidar (**2**) was a dual ABCG2 and ABCC1 inhibitor, but showed much higher inhibitory potency and also higher efficacy at the ABCB1 than at the ABCG2 transporter. Structural modifications at the benzamide core of **2** led to a drastic increase in selectivity for ABCG2 over ABCB1 (compound **9**), confirming our previous results [40]. Compound **9** showed only very low inhibition of ABCB1, but inhibited ABCG2 with an  $IC_{50}$  value of 101 nM. The maximal response of 99% was higher than that determined in the flow cytometric mitoxantrone efflux assay we used before. The replacement of the labile amide moiety in **9** by a triazole ring resulted in the novel inhibitors **38-42**. This replacement was well-tolerated, the efficacy of the new compounds being 85-95% and the potencies in the three-digit nanomolar range. Apparently the length of the linker between the tetrahydroisoquinoline moiety and the phenyl ring does not clearly correlate with the inhibitory activity. Compounds **38** and **41**, as well as **39** and **42**, only differ in the length of the linker (one vs. two methylene groups). Whereas compounds **39** and **42** were equipotent ( $IC_{50}$  values of about 150 nM), compound **38** ( $IC_{50}$  of 350 nM) was almost twice as potent as **41**. The introduction of a PEG chain increased the potency by a factor of two (**38** vs. **39**) or four (**41** vs. **42**). The replacement of the two methoxy groups at the tetrahydroisoquinoline moiety by hydrogen atoms (**40**) increased the potency slightly. Taken together, variations in the linker and the moieties attached to the tetrahydroisoquinoline ring seem to be well-tolerated. In terms of selectivity, compounds **38-42** showed great differences. While all of them were inactive at ABCC1, they showed very dissimilar effects on ABCB1. Here again, there was no correlation between the length of the linker and ABCB1 inhibition. Both **38** and **39**, with an identical linker (one methylene group), inhibited ABCB1 with a maximal response between 20% and 30% (up to 100  $\mu$ M). **40**, **41** and **42** (two methylene groups) diverged very much depending on the substituents at the tetrahydroisoquinoline moiety. **41** was inactive, **40** was 11% effective (up to 100  $\mu$ M) and **42**, containing the PEG chain, was 80% effective and exhibited an  $IC_{50}$  value in the low micromolar range, making it a dual ABCG2 and ABCB1 inhibitor. It seems as if the PEG chain can confer activity at ABCB1. Since, however, this was not the case for **39** as compared to **38**, this effect appears to depend on the specific structure.

**Table 1.** Inhibitory effect of the reference compounds **2-8**, our previous tariquidar analog **9** and the new inhibitors **38-42** and **56-59** on the transport activity of ABCG2, ABCB1 and ABCC1.


n=1	n=2	R <sup>1</sup>	R <sup>2</sup>	R <sup>3</sup>
<b>38</b>	<b>40</b>	H	H	OMe
<b>39</b>	<b>41</b>	OMe	OMe	OMe
	<b>42</b>	O(CH <sub>2</sub> CH <sub>2</sub> O) <sub>3</sub> Me	OMe	OMe
	<b>56</b>	OMe	OMe	Me
	<b>57</b>	OMe	OMe	Et
	<b>58</b>	OMe	OMe	iPr
	<b>59</b>	O(CH <sub>2</sub> CH <sub>2</sub> O) <sub>3</sub> Me	OMe	Et

Compound	ABCG2 <sup>a</sup>		ABCB1 <sup>b</sup>		ABCC1 <sup>c</sup>	
	IC <sub>50</sub> [nM] <sup>d</sup>	I <sub>max</sub> [%] <sup>d,e</sup>	IC <sub>50</sub> [nM] <sup>d</sup>	I <sub>max</sub> [%] <sup>d,f</sup>	IC <sub>50</sub> [nM] <sup>d</sup>	I <sub>max</sub> [%] <sup>d,g</sup>
<b>2</b> (tariquidar)	6223 ± 707	72 ± 3	356 ± 3	100 ± 3	inactive <sup>h,i</sup>	–
<b>3</b> (FTC)	1483 ± 194	102 ± 3	inactive	–	inactive	–
<b>4</b> (Ko143)	92 ± 9	116 ± 2	≥ 25520 <sup>j</sup>	≥ 11	6650 ± 2856	29 ± 8
<b>5</b>	1115 ± 32	111 ± 3	inactive	–	inactive	–
<b>6</b>	1800 ± 300 <sup>i</sup>	108 ± 5 <sup>i</sup>	inactive <sup>i</sup>	–	inactive <sup>i</sup>	–
<b>7</b>	707 ± 98	109 ± 12	6756 ± 946	10 ± 1	3599 ± 302	15 ± 1
<b>8</b> (YHO-13177)	3345 ± 342	106 ± 9	≥ 65480	≥ 53	≥ 39750	≥ 81
<b>9</b> (UR-ME22-1)	101 ± 17	99 ± 1	≥ 12080	≥ 14	inactive	–
<b>38</b> (UR-MB86)	350 ± 53	87 ± 2	≥ 10730	≥ 25	inactive	–
<b>39</b> (UR-MB84)	153 ± 12	85 ± 3	≥ 25030	≥ 21	inactive	–
<b>40</b> (UR-MB81)	486 ± 5	95 ± 5	≥ 38270	≥ 11	inactive	–
<b>41</b> (UR-MB19)	617 ± 179	90 ± 3	inactive	–	inactive	–
<b>42</b> (UR-MB95)	144 ± 35	86 ± 3	1623 ± 405	80 ± 7	inactive	–
<b>56</b> (UR-St1)	140 ± 40	97 ± 2	inactive	–	inactive	–
<b>57</b> (UR-MB108)	79 ± 5	91 ± 2	inactive	–	inactive	–
<b>58</b> (UR-St2)	295 ± 28	90 ± 0.4	≥ 21830	≥ 24	≥ 19040	≥ 14
<b>59</b> (UR-MB136)	81 ± 16	90 ± 3	≥ 44460	≥ 42	inactive	–

<sup>a</sup> Hoechst 33342 microplate assay using ABCG2-expressing MCF-7/Topo cells.<sup>b</sup> Calcein-AM microplate assay using ABCB1-expressing KB-V1 cells.<sup>c</sup> Calcein-AM microplate assay using ABCC1-expressing MDCK.2-MRP1 cells.<sup>d</sup> Mean values ± SEM from two to seven independent experiments, each performed in triplicate.<sup>e</sup> Maximal inhibitory effect (I<sub>max</sub>) relative to the response to FTC at a concentration of 10 μM (100%).<sup>f</sup> Maximal inhibitory effect (I<sub>max</sub>) relative to the response to tariquidar at a concentration of 10 μM (100%).<sup>g</sup> Maximal inhibitory effect (I<sub>max</sub>) relative to the response to reversan at a concentration of 30 μM (100%).<sup>h</sup> Inactive: response ≤ 10% up to a concentration of 100 μM.<sup>i</sup> Data taken from our previous studies [46].<sup>j</sup> No plateau was reached up to a concentration of 100 μM. In these cases, minimum IC<sub>50</sub> values and I<sub>max</sub> values were stated.

The second modification of **9** was the replacement of the labile ester moiety at the central, trisubstituted phenyl core by ketones, yielding the inhibitors **56-59**. This alteration increased the efficacy at ABCG2 to 90-97%. The IC<sub>50</sub> values were quite similar in the two to three digit nanomolar range. The length of the acyl group attached to the benzamide core was varied. The propionyl group (in **57**) proved to be superior to the smaller acetyl group (in **56**) and also to the bulkier isobutyryl moiety (in **58**) in terms of inhibitory potency and selectivity, **58**

showing moderate ABCB1 and ABCC1 activity. In this subseries, the introduction of a PEG chain (**59**) left the inhibitory potency at ABCG2 unchanged, but, here again, caused an inhibitory effect on ABCB1, with the maximal response being 42% (up to a concentration of 100  $\mu$ M). It is conceivable that the PEG chain confers affinity to the binding site in ABCB1. Except for **58**, none of the ketone-containing inhibitors showed inhibition of ABCC1.

### **2.3 Effect on the ABCG2 ATPase Activity**

On the basis of the results obtained from the functional transport assays, the two most potent novel inhibitors (**57** and **59**), their precursor **9** and the reference compounds **2-8** were examined with regard to their effect on ABCG2 ATPase activity. The ATPase assay, requiring relatively high levels of transporter protein, was performed with ABCG2-expressing Sf9 membranes. ABC transporters gain the energy for the transport of their substrates from ATP hydrolysis to ADP and inorganic phosphate. The latter was determined in a colorimetric reaction after incubation of the membrane preparations with different concentrations of test compounds, resulting in concentration-response curves (examples depicted in Figure 4A+B). In a variant of this assay, the ABCG2 transporters in the membranes were additionally stimulated with the ABCG2 substrate sulfasalazine to investigate whether the test compounds reverse the activating effect caused by sulfasalazine, or not (Figure 4C+D). The results of the two assay variants are summarized in Table 2.

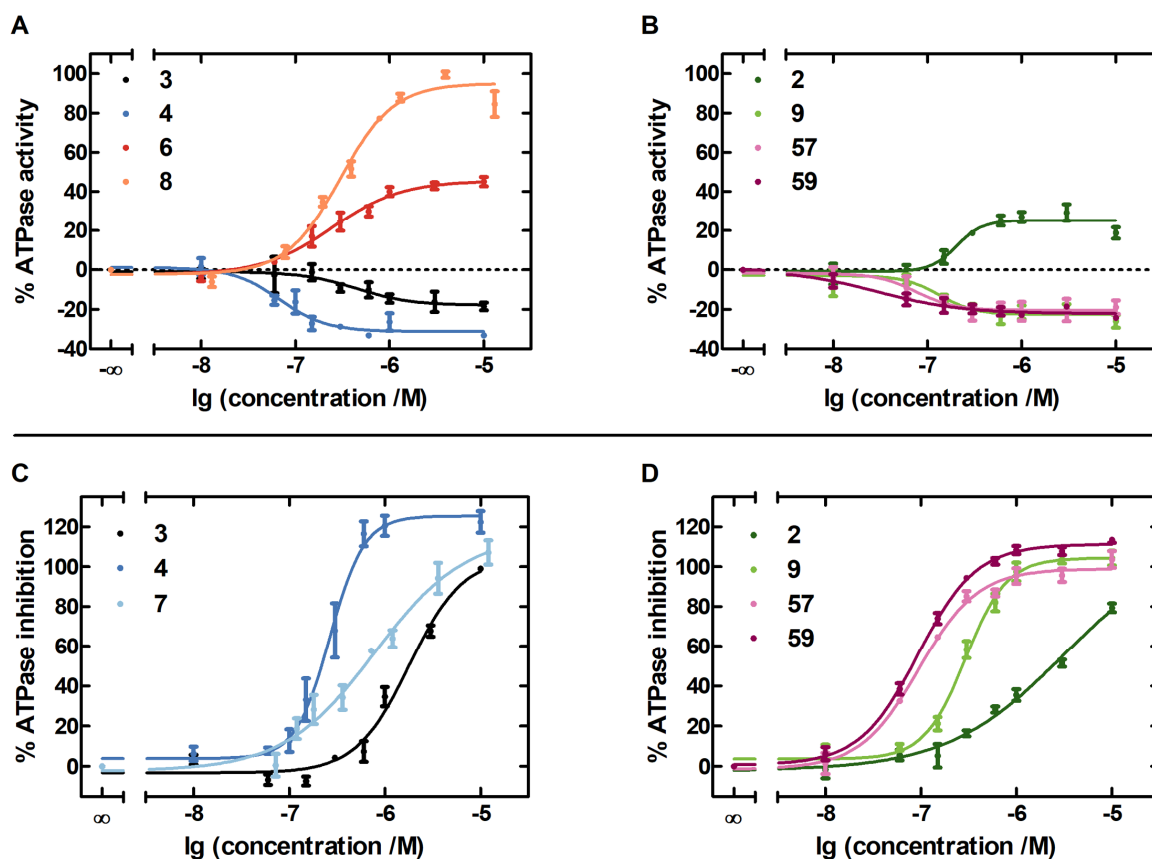
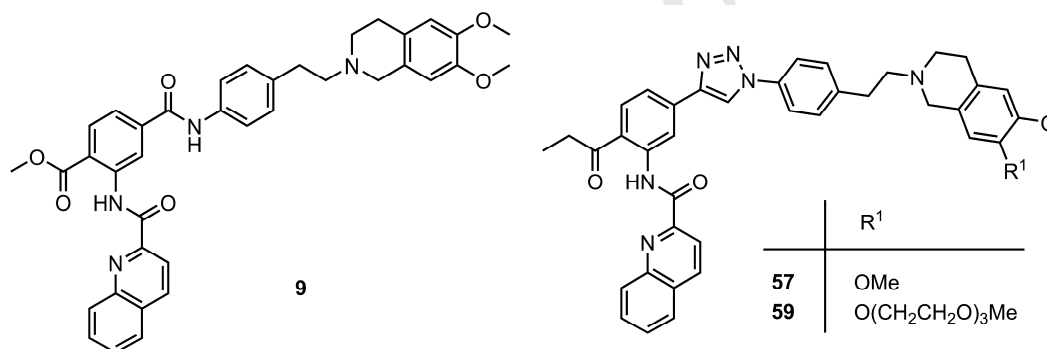


**Figure 4.** (A+B) Concentration-dependent stimulation or suppression of the ATPase activity in ABCG2-expressing Sf9 membranes by (A) the reference compounds FTC (3), Ko143 (4), 6 and 8 as well as (B) tariquidar (2), its analog UR-ME22-1 (9) and its novel analogs 57 and 59. The effect is expressed relative to the basal ATPase activity (0%) and the maximal stimulatory effect in the presence of 30  $\mu$ M sulfasalazine set to 100%. (C+D) Concentration-dependent inhibition of the sulfasalazine (3  $\mu$ M) -stimulated ATPase activity in ABCG2-expressing Sf9 membranes by (C) the reference compounds FTC (3), Ko143 (4) and 7 as well as (D) tariquidar (2), its analog UR-ME22-1 (9) and its novel analogs 57 and 59. The inhibition is expressed relative to the maximal inhibitory effect in the presence of 10  $\mu$ M FTC set to 100%.

In the absence of inhibitors, ABCG2 showed relatively high basal ATPase activity, which was set to zero in our assay. The test compounds, all being transport inhibitors, behaved in three different manners with respect to ABCG2 ATPase activity. Firstly, most of them decreased it to a level below the basal activity (below zero) or secondly had no effect on it. In these two cases it can be assumed that the test compounds are not transported and the inhibition of the transport of other substrates may be, at least in part, attributed to the inhibition of the ATPase activity of the transporter. A reduction of the ATPase activity was evoked by FTC (3) and its analogs Ko143 (4) and 5, and the tariquidar analogs 9, 57 and 59, their maximal effects being between -20% and -37% and their inhibitory potencies in the two-digit (4, 57 and 59) to three-digit (3, 5 and 9) nanomolar range. The compounds were also able to inhibit sulfasalazine-stimulated ATPase activity with an efficacy around 100% (3, 9, 57 and 59) or more (4, 5) and potencies again in the two-digit (57 and 59) to three digit (4, 5 and 9) nanomolar range. Only 3 shows a higher  $IC_{50}$  value of 1.8  $\mu$ M. The chromone 7 exhibited no effect on the basal ATPase activity, but was able to reverse activation by sulfasalazine.

Thirdly, some compounds increased the ATPase activity and can therefore be considered transporter substrates, although the coupling of ATP-hydrolysis to transport has been challenged [47]. It is conceivable that transport inhibitors that are strong ATPase activators at the same time compete with other substrates, e.g. Hoechst 33342, for transport by diffusing rapidly back into the cell (so-called “fast-diffusers”) [48]. To explore if they also compete for the same binding site, further interaction type analyses would be required. It seems probable, though, because we recently identified one central multidrug-binding site [39] (i.e. for substrates and inhibitors). The acrylonitrile **8** activated the ATPase activity as efficiently as the standard activator sulfasalazine (namely with 99%) and even exhibited a lower EC<sub>50</sub> value (327 nM vs. 916 nM for sulfasalazine). Compound **8** might be such a “fast-diffuser”, an assumption also supported by its low molecular mass.

**Table 2.** Effect of the reference compounds **2-8**, our previous tariquidar analog **9** and the new inhibitors **57** and **59** on the ATPase activity of ABCG2 with and without pre-stimulation with sulfasalazine.



Compound	Effect on ATPase activity <sup>a</sup>		Inhibition on stimulated ATPase activity <sup>b</sup>	
	EC <sub>50</sub> [nM] <sup>c,d</sup>	E <sub>max</sub> [%] <sup>c,e</sup>	IC <sub>50</sub> [nM] <sup>c</sup>	I <sub>max</sub> [%] <sup>c,f</sup>
Sulfasalazine	916 ± 2	96 ± 4	–	–
<b>2</b> (tariquidar)	211 ± 31	25 ± 3	≥ 1180	≥ 79
<b>3</b> (FTC)	412 ± 240	- 20 ± 2	1808 ± 203	104 ± 2
<b>4</b> (Ko143)	70 ± 17	- 31 ± 1	271 ± 44	124 ± 5
<b>5</b>	134 ± 3	- 37 ± 2	226 ± 30	141 ± 8
<b>6</b>	274 ± 86	45 ± 3	194 ± 128	19 ± 4
<b>7</b>	–	0 ± 1	745 ± 74	113 ± 4
<b>8</b> (YHO-13177)	327 ± 34	99 ± 7	–	–
<b>9</b> (UR-ME22-1)	105 ± 14	- 27 ± 7	294 ± 17	105 ± 3
<b>57</b> (UR-MB108)	70 ± 28	- 21 ± 4	96 ± 2	99 ± 3
<b>59</b> (UR-MB136)	52 ± 38	- 23 ± 0.1	93 ± 8	112 ± 1

<sup>a</sup> ATPase microplate assay using ABCG2-expressing Sf9 membranes.

<sup>b</sup> ATPase microplate assay using ABCG2-expressing Sf9 membranes stimulated with sulfasalazine at a concentration of 3 μM.

<sup>c</sup> Mean values ± SEM from two to four independent experiments, each performed in duplicate.

<sup>d</sup> Half-maximal effective concentrations were termed EC<sub>50</sub> (not IC<sub>50</sub>) values, even if the ATPase activity was reduced, in order to avoid confusion with the data from the ATPase assay with sulfasalazine stimulation.

<sup>e</sup> Maximal effect (E<sub>max</sub>) on the ATPase activity relative to the basal ATPase activity (0%) and to the response to sulfasalazine at a concentration of 30 μM (100%).

<sup>f</sup> Maximal inhibitory effect (I<sub>max</sub>) relative to the response to FTC at a concentration of 10 μM (100%).

Transport inhibitors that exert only a partially activating effect on the ATPase activity were tariquidar (**2**), showing a maximal effect of 25% and standing in contrast with its ATPase-suppressing analogs (**9**, **57** and **59**), and the chromone **6** (45%), as opposed to the chromone **7** with no effect. Nonetheless, both **2** and **7** were able to partly antagonize ATPase stimulation by sulfasalazine.

The ATPase results from our novel tariquidar derivatives are consistent with the structural data on ABCG2 inhibition we published recently [39]. We showed that compound **59** and a derivative of **4** both bound to the multidrug-binding site identified in these experiments (cavity 1; located in the transmembrane domains) and locked the inward-facing conformation, thereby inhibiting the ATPase activity (of the cytoplasmic, nucleotide-binding domains) due to conformational coupling.

Figure 5 shows the compartment of the reference compounds FTC (**3**) and its analogs Ko143 (**4**) and **5**, in relation to our previous tariquidar analog **9** and our most potent novel analogs **57** and **59**, all of which suppressed the ABCG2 ATPase activity. Depicted are half-maximal (effective or inhibitory) concentrations, determined in the three different functional assays performed, namely the Hoechst 33342 transport assay and the ATPase assay with and without pre-stimulation with sulfasalazine. Of course, it is expected that half-maximal concentrations differ when determined in different assays, depending on the experimental conditions. However, the differences in the experimental setup should become obvious by a constant factor between the  $IC_{50}/EC_{50}$  values from the different assays, provided that all compounds share the same mechanism of action. To identify outliers and to show commonality, we plotted the functional data obtained from different assays in a radar chart. Ko143 (**4**) and the tariquidar analogs **9**, **57** and **59** showed similar behavior – their potencies in the three assays coincided fairly well. FTC (**3**) and its derivative **5** on the other hand, did not show comparable half-maximal concentrations. Their potencies determined in the Hoechst transport assay were much higher than those in the ATPase assay and compound **3** also showed a higher half-maximal concentration in the ATPase assay with sulfasalazine-stimulation than without. Our previous structural study [39] showed that one **59** molecule or two molecules of a derivative of **4** completely occupied the volume of cavity 1. We concluded that these inhibitors act competitively at the binding site with substrates, which was the second inhibition mechanism identified, apart from ATPase inhibition. So one could speculate that not only **59** but also the other inhibitors compete for the binding site with substrates, and similar potencies in the three assays might suggest that the inhibitors **4**, **9**, **57** and **59** bind to ABCG2 with higher affinities than the substrates Hoechst 33342 and sulfasalazine. Vice versa, higher potencies in assays in

the presence of substrates might be taken as a hint to displacability of **3** and **5** by the respective substrates at the concentrations employed.

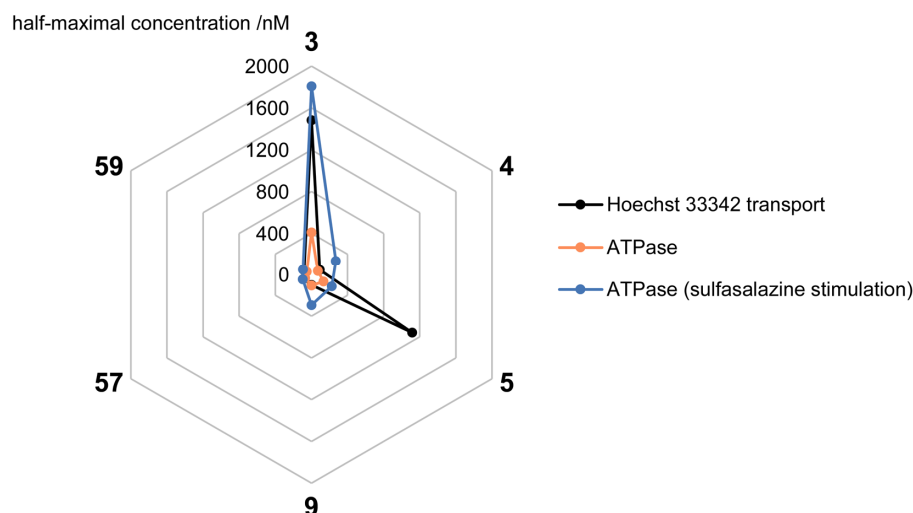


**Figure 5.** Comparison of half-maximal effective/ inhibitory concentrations produced by the compounds **3**, **4**, **5**, **7**, **9**, **57** and **59** in the Hoechst 33342 transport assay (black), the ATPase assay (orange) and the ATPase assay with pre-stimulation with sulfasalazine (blue).

## 2.4 Thermostabilization of ABCG2

We analyzed the thermostabilization of ABCG2 by our two most potent novel tariquidar analogs (**57** and **59**) and the reference compound Ko143 (**4**) in a size-exclusion chromatography-based thermostability assay (SEC-TS). For this purpose, purified ABCG2 was incubated with or without inhibitor at increasing temperatures and subjected to SEC. The main peak heights were plotted against the temperature to obtain the “melting points” ( $T_m$  values) of ABCG2. The curves for ABCG2 in the presence and absence of compound **57** are depicted in Figure 6; the curves for ABCG2 in the presence and absence of compounds **4** and **59** were included in our previous report [39] (on the cryo-EM structure of ABCG2 in complex with inhibitors).

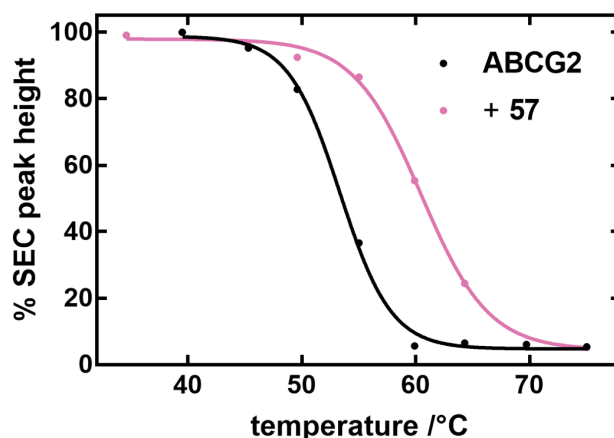


**Figure 6.** SEC-TS of ABCG2 before or after the addition of **57** at a concentration of 10  $\mu$ M. The peak heights are expressed relative to the peak height of ABCG2 without inhibitor at 4 °C (HP-SEC analysis, UV detection at 280 nm).

The melting points determined in this assay are listed in Table 3. Compounds **4**, **57** and **59** showed approximately 7 °C thermostabilization of purified ABCG2. Since the three compounds stabilized ABCG2 to the same extent, it can be deduced that these compounds bind to ABCG2 with similar affinities.

**Table 3.**  $T_m$  values of ABCG2 alone and in complex with **4**, **57** or **59** determined in a SEC-TS.

sample	$T_m$ [°C] <sup>a</sup>
ABCG2	53.3 ± 0.3
<b>4</b> (Ko143)	60.0 ± 0.3
<b>57</b> (UR-MB108)	60.5 ± 0.3
<b>59</b> (UR-MB136)	59.0 ± 0.5

<sup>a</sup> Best fit values ± SD.

## 2.5 Cytotoxicity and Reversal of Drug Resistance

The effect of the two most potent novel transport and ATPase inhibitors (**57** and **59**) and the most potent reference compound Ko143 (**4**) on the proliferation as well as the ability to overcome drug resistance of MCF-7/Topo cells were investigated in a kinetic chemosensitivity assay, using the inhibitors alone and in combination with the cytostatic topotecan, an ABCG2 substrate. The results are shown in Figure 7. Incubation of the cells with **4** had no effect on cell proliferation up to a concentration of 3 µM. A slight cytotoxic effect was observed at a concentration of 10 µM. When incubated with topotecan alone at a concentration of 100 nM, the cells were not affected due to their resistance against the cytostatic. By contrast, the combination of 100 nM topotecan with a per se nontoxic concentration of **4** led to a complete reversal of resistance. Inhibitor **57** was nontoxic up to a concentration of 1 µM. At higher concentrations, however, it showed cytotoxicity, which might be an interesting property in view of addressing tumor stem cells [49]. By analogy with **4**, **57** reversed topotecan resistance when administered at nontoxic concentrations in combination with the cytostatic (100 nM). The inhibitor **59**, which only differs from **57** in the PEG chain attached to the tetrahydroisoquinoline moiety, was also able to reverse drug resistance in MCF-7/Topo cells and was superior to **57** in so far as it did not exhibit marked cytotoxicity at concentrations up to 10 µM.

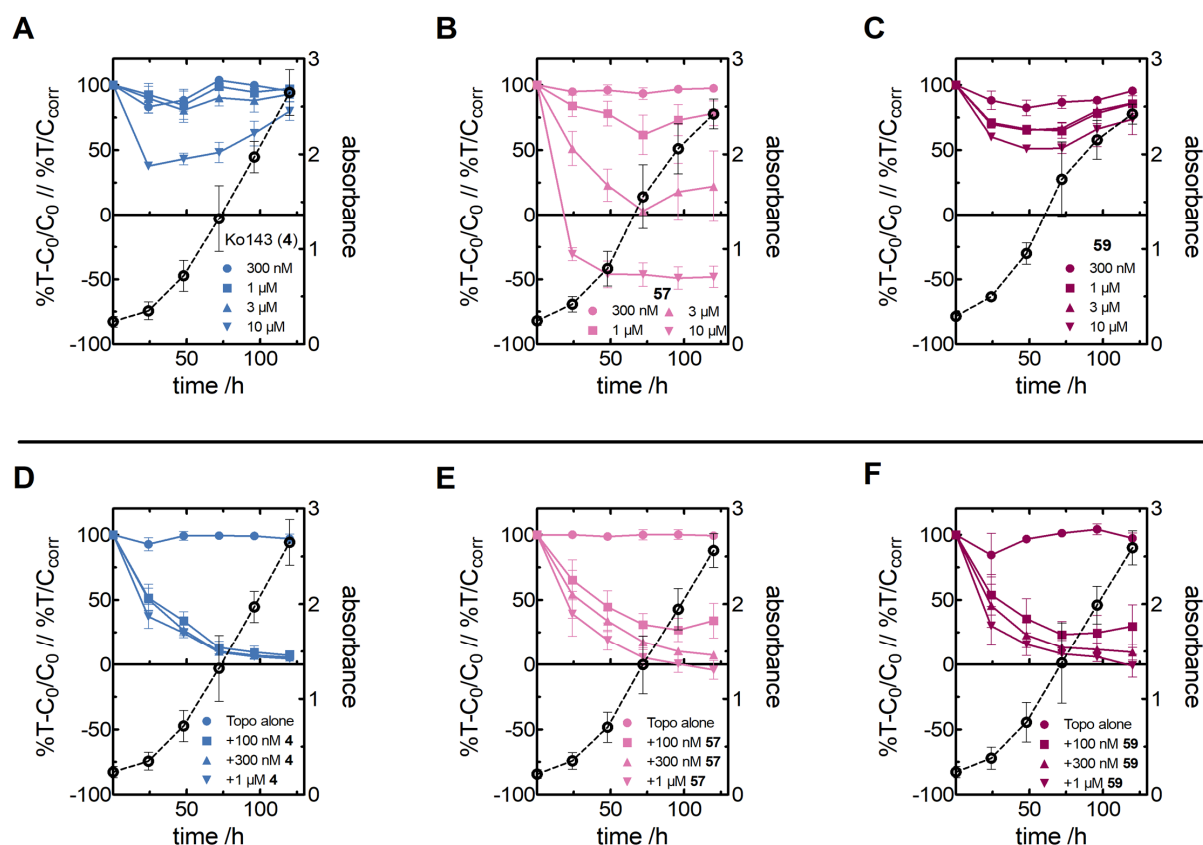


**Figure 7.** (A-C) Antiproliferative activities of Ko143 (**4**) (A) and the novel tariquidar analogs **57** (B) and **59** (C) against MCF-7/Topo cells upon long-term incubation. (D-F) Reversal of ABCG2-mediated drug resistance against topotecan on proliferating MCF-7/Topo cells: effect of 100 nM topotecan (Topo) alone and in combination with different concentrations of **4** (D), **57** (E) or **59** (F). Antiproliferative effects correspond to the left y-axes. The growth curves of untreated control cells (open circles) correspond to the right y-axes. Data are mean values  $\pm$  SEM of two to four independent experiments, each performed in octuplicate.

In conclusion, the reversal of drug resistance in MCF-7/Topo cells by the compounds **4**, **57** and **59** is in good agreement with the data from the transport assays (Figure 3, Table 1) and confirms the three substances as inhibitors of ABCG2-mediated drug efflux.

## 2.6 Stability in Blood Plasma

Prerequisite for in vivo studies is the stability of the test compounds in blood plasma. We first replaced the labile benzamide bond in **9** by a triazole core (affording compounds **38-42**) and then introduced ketones at the central trisubstituted phenyl ring as alternatives to the labile ester moiety, resulting in the inhibitors **56-59**. Exemplarily, the stability of **59** upon incubation in murine blood plasma at 37 °C was demonstrated by HPLC-analysis. As depicted in Figure 8, the peak area of **59** remains virtually unchanged over a period of 24 hours and no additional peaks were detected at 220 nm. This experiment demonstrates that the bioisosteric replacement of the labile amide and ester moieties in **9** provided for stable inhibitors.

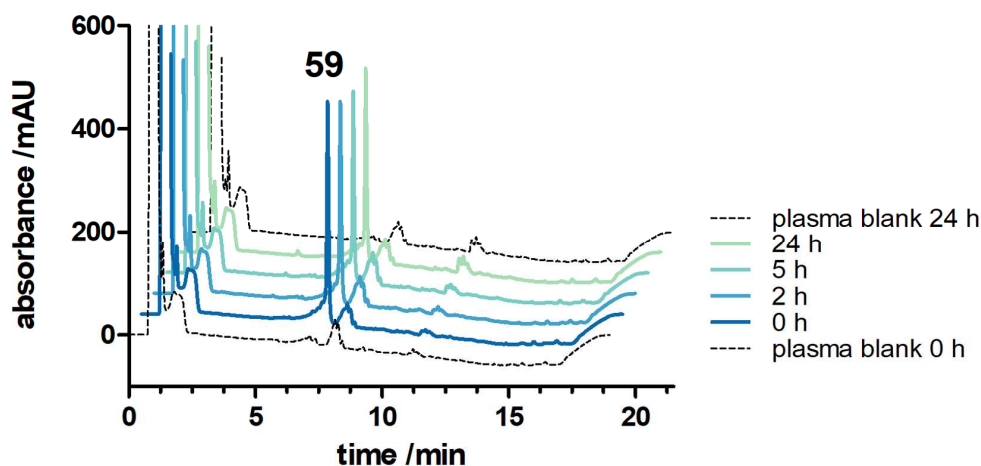


**Figure 8.** Chromatograms illustrating the stability of compound **59** upon incubation in murine blood plasma at 37 °C over a period of 24 h. RP-HPLC analysis, UV detection at 220 nm.

### 3 Conclusion

The study presented is a continuation of our previous investigations on tariquidar analogs as ABCG2 inhibitors. Among the title compounds, UR-MB108 (**57**) and UR-MB136 (**59**) excelled in terms of inhibitory potency in the Hoechst 33342 transport assay. With  $IC_{50}$  values of around 80 nM, they are among the most potent ABCG2 inhibitors known so far. Reversal of drug resistance in MCF-7/Topo breast cancer cells confirmed their ability to inhibit drug efflux. The PEGylated compound **59** also showed low activity at ABCB1, whereas **57** was highly ABCG2-selective. Both compounds suppressed the basal ABCG2 ATPase activity and were able to antagonize the ATPase-activating effect of sulfasalazine. Furthermore, the two compounds thermostabilized ABCG2 to the same extent, suggesting comparable binding affinities. Compound **59** was already analyzed in our precedent structural study [39] of ABCG2 in complex with inhibitors (but its synthesis and biological characterization has not been described until this report). We showed that one **59** molecule occupied the cavity for multidrug binding (in the transmembrane domain), locked the inward-facing conformation and inhibited the cytosolic ATPase subunit via conformational coupling. Compounds **57** and **59** differ only in the PEG chain attached at the tetrahydroisoquinoline moiety in **59** and it is probable that they bind similarly to the central multidrug binding site, an assumption which is supported by their same behavior in the functional assays and the thermostability assay.

Respecting future research, we expect compounds **57** and **59** to be of potential value as reference substances in mechanistic studies on ABCG2 regarding transport and inhibition. Compound **57** is beneficial, because it is more conveniently synthesized than **59**. Furthermore, in the light of their stability in blood plasma, compounds **57** and **59** can be employed as pharmacological tools for in vivo investigations on the (patho-)physiological role of the

ABCG2 transporter and as a means to overcome MDR and the BBB. The high specificity of compound **57** towards ABCG2 makes it convenient, for instance, as PET tracer for imaging the ABCG2 transporter at the BBB, the two methoxy groups in **57** being suited for  $^{11}\text{C}$ -PET labeling. In addition, it could be used for in vivo studies with pharmacological interventions specifically on the ABCG2 isoform, for example to improve the efficacy of photodynamic therapy of non-melanoma skin cancer.

## 4 Experimental Section

### 4.1 Chemistry: Experimental Protocols

#### 4.1.1 General Experimental Conditions

**Chemicals and solvents** were purchased from commercial suppliers (Sigma Aldrich, Munich, Germany; Merck, Darmstadt, Germany; VWR, Darmstadt, Germany; Thermo Fisher Scientific, Waltham, MA, USA; TCI, Eschborn, Germany) and used without further purification unless stated otherwise. The catalyst  $\text{Pd}(\text{PPh}_3)_2\text{Cl}_2$  [50] for the Sonogashira couplings and the ligand tris[(1-benzyl-1*H*-1,2,3-triazol-4-yl)methyl]amine [43] (TBTA) for the CuAAC were synthesized according to published procedures. Per analysis grade solvents were used for reaction mixtures and technical grade solvents for chromatography (automated flash column chromatography and TLC). Reactions requiring anhydrous conditions were carried out in dried reaction vessels under an atmosphere of nitrogen and anhydrous solvents were used. Millipore water was used throughout for the preparation of buffers and HPLC eluents. Acetonitrile for analytical and preparative HPLC (gradient grade) was obtained from Merck (Darmstadt, Germany).

**Thin layer chromatography** was performed on TLC Silica gel 60 F<sub>254</sub> aluminium plates (Merck, Darmstadt, Germany). Visualization was accomplished by UV irradiation at wavelengths of 254 nm and 366 nm or by staining with potassium permanganate or Ehrlich's reagent.

**Automated flash column chromatography** was performed on an Isolera Spektra One device (Biotage, Uppsala, Sweden). Silica gel 60 (0.040-0.063 mm) for flash column chromatography (Merck, Darmstadt, Germany) was used.

**Melting points** were determined in open capillaries on an OptiMelt MPA 100 apparatus (Stanford Research Systems, Sunnyvale, CA, USA) and are uncorrected.

**NMR spectra** were recorded on an Avance 300 instrument (7.05 T,  $^1\text{H}$ : 300.1 MHz,  $^{13}\text{C}$ : 75.5 MHz), an Avance 400 instrument (9.40 T,  $^1\text{H}$ : 400 MHz,  $^{13}\text{C}$ : 101 MHz) or an Avance

600 instrument with cryogenic probe (14.1 T,  $^1\text{H}$ : 600 MHz,  $^{13}\text{C}$ : 151 MHz) (Bruker, Karlsruhe, Germany) with TMS as external standard.

**High-resolution mass spectrometry (HRMS)** analysis was performed on an Agilent 6540 UHD Accurate-Mass Q-TOF LC/MS system (Agilent Technologies, Santa Clara, CA, USA), using an ESI source.

**IR spectra** were recorded with a Golden Gate Single Reflection Diamond ATR System (Specac, Orpington, UK) in an Excalibur FTS 3000 FT-IR-Spectrometer (Bio-Rad, München, Germany).

**Preparative HPLC** was performed on a system from Knauer (Berlin, Germany), consisting of two K-1800 pumps and a K-2001 detector. A Kinetex<sup>®</sup> XB-C18 (5  $\mu\text{m}$ , 100  $\text{\AA}$ , 250 mm x 21.2 mm; Phenomenex, Aschaffenburg, Germany) served as RP-column at a flow-rate of 15 mL/min. Mixtures of acetonitrile and 0.1% aq TFA were used as mobile phase. The detection wavelength was set to 220 nm throughout. The solvent mixtures were removed by lyophilization, using an Alpha 2-4 LD lyophilisation apparatus (Christ, Osterode am Harz, Germany) equipped with an RZ 6 rotary vane vacuum pump (Vacuubrand, Wertheim, Germany).

**Analytical HPLC** was performed on a system from Agilent Technologies (Santa Clara, CA, USA) (Series 1100) composed of a G1312A binary pump equipped with a G1379A degasser, a G1329A ALS autosampler, a G1316A COLCOM thermostated column compartment and a G1314A VWD detector. A Kinetex<sup>®</sup> C8 (2.6  $\mu\text{m}$ , 100  $\text{\AA}$ , 100 mm  $\times$  4.6 mm; Phenomenex, Aschaffenburg, Germany) served as RP-column at a flow rate of 1 mL/min. Oven temperature was set to 30  $^\circ\text{C}$  throughout. Mixtures of acetonitrile (A) and 0.05% aq TFA (B) were used as mobile phase. The detection wavelength was set to 220 nm throughout. Solutions for injection (40  $\mu\text{M}$ ) were prepared by diluting a stock solution in DMSO with a mixture of A and B corresponding to the mixture at the start of the gradient. The injection volume was 50  $\mu\text{L}$ . The following linear gradient was applied: 0-12 min: A/B 30:70-95:5, 12-15 min: A/B 95:5.

#### 4.1.2 General Procedure for N-Alkylation

The 1,2,3,4-tetrahydroisoquinoline derivative (1 eq), 1-(bromomethyl)-4-nitrobenzene (1 eq) or 1-(2-bromoethyl)-4-nitrobenzene (1 eq) and  $\text{K}_2\text{CO}_3$  (3 eq) were refluxed in MeCN overnight. The reaction mixture was cooled to rt, filtered and the filtrate concentrated under reduced pressure. The residual solid was taken up in DCM and washed with  $\text{H}_2\text{O}$  twice. The organic layer was dried over  $\text{MgSO}_4$ , the solvent removed under reduced pressure and the residue purified by flash column chromatography.

### 4.1.3 General Procedure for the Reduction of Nitro Compounds

The nitrobenzene derivative (1 eq) was dissolved in EtOH, a 10% Pd/C catalyst (10 wt%) was added and the suspension was stirred rapidly in a hydrogen atmosphere (40 bar) at rt overnight. The catalyst was filtered off, the solvent was evaporated and the residue was subjected to flash column chromatography.

### 4.1.4 General Procedure for Azide Formation

The amine (1 eq) was dissolved in 6 M HCl aq and cooled to -5 °C. An aqueous solution of NaNO<sub>2</sub> (1.0 eq) was added and the mixture was stirred for 1 h. The solution was neutralized with an aqueous solution of NaOAc while being cooled continuously. An aqueous solution of NaN<sub>3</sub> (1.2 eq) was added dropwise. After another h of cooling, the mixture was slowly warmed to rt, and the product was extracted with EtOAc. The combined organic layers were washed with H<sub>2</sub>O and brine, dried over MgSO<sub>4</sub> and concentrated. The product was used for subsequent conversion without further purification.

### 4.1.5 General Procedure for the Ortho Acylation of 3-Bromoaniline

To a cooled (0 °C) solution of BCl<sub>3</sub> (1 M solution in heptane, 1.1 eq) in DCM 3-bromoaniline (1 eq) was added under a stream of nitrogen gas. The mixture was stirred for 20 min and AlCl<sub>3</sub> (1.1 eq) and propionitrile (1 eq) were added subsequently. Stirring continued for 24 h under reflux. After cooling to 0 °C, 2 M HCl aq was added. The mixture was stirred rapidly for 10 min and heated again to 80 °C for 1 h. The product was extracted with DCM and the organic phase washed with 1 M NaOH aq, dried and concentrated. The residue was subjected to flash column chromatography.

### 4.1.6 General Procedure for the Sonogashira Reaction

The bromobenzene derivative (1 eq), CuI (0.1 eq) and Pd(PPh<sub>3</sub>)<sub>2</sub>Cl<sub>2</sub> (0.05 eq) were placed in a sealed vial under nitrogen. A mixture of degassed THF and NEt<sub>3</sub> (2:1) and ethynyltrimethylsilane (1.5 eq) was added. The solution was stirred at 60 °C overnight. H<sub>2</sub>O was added and the product was extracted with DCM. The organic phase was separated, concentrated and purified by flash column chromatography.

### 4.1.7 General Procedure for TMS Deprotection

A solution of the respective trimethylsilyl-protected alkyne (1 eq) in THF was cooled in an ice bath. Under stirring, TBAF (1.5 M in THF, 1.5 eq) was added and stirring was continued until TLC analysis revealed complete consumption of the starting material (approximately 2 h). The solvent was evaporated, saturated NH<sub>4</sub>Cl solution was added and the compound extracted with DCM. The organic layer was separated, dried over Mg<sub>2</sub>SO<sub>4</sub> and the solvent was

evaporated. In case of sufficient purity the product was used for subsequent reaction without further purification. Otherwise, flash column chromatography was used to remove traces of the starting material.

#### 4.1.8 General Procedure for Amide Formation

DIPEA (10 eq), HBTU (3 eq) and quinoline-2-carboxylic acid (3 eq) were dissolved in anhydrous DCM under a nitrogen atmosphere and cooled to 0 °C. The amine derivative was added in small portions and the mixture was allowed to reach rt and stirred for 24 h. The solution was washed with H<sub>2</sub>O and brine, twice each, dried and concentrated. The residue was subjected to flash column chromatography.

#### 4.1.9 General Procedure for the CuAAC

The azide (1.0-1.5 eq), the alkyne (1.0-1.3 eq), CuSO<sub>4</sub> · 6H<sub>2</sub>O (0.1 eq), sodium ascorbate (0.5 eq) and TBTA (0.1 eq) were dissolved in DMF or, in case of UR-St1 and UR-St2, in THF and stirred for 24 h under a nitrogen atmosphere. DCM was added and the organic layer was washed with H<sub>2</sub>O, dried over MgSO<sub>4</sub> and concentrated. The crude mixture was purified by flash column chromatography.

### 4.2 Biological Assays: Experimental Protocols

#### 4.2.1 General Experimental Conditions

**Materials.** Commodity chemicals and solvents were purchased from commercial suppliers (Sigma Aldrich, Munich, Germany; Merck, Darmstadt, Germany; VWR, Darmstadt, Germany; Thermo Fisher Scientific, Waltham, MA, USA; Invitrogen, Karlsruhe, Germany). Topotecan and vinblastine were obtained from Sigma Aldrich. Hoechst 33342 and calcein-AM were procured from Biotium (Fremont, CA, USA). FTC was from Merck. Tariquidar was synthesized in our laboratory according to literature[21] with slight modifications[51]. Reversan was obtained from Tocris (Wiesbaden-Nordenstadt, Germany). Cholesterol/RAMEB, a complex of 5.4% cholesterol and randomly methylated  $\beta$ -cyclodextrin, was acquired from CycloLab (Cyclodextrin Research and Development Laboratory, Budapest, Hungary). Millipore water was used throughout for the preparation of buffers, aqueous reagent solutions and HPLC eluents. The pH of buffers and aqueous reagent solutions was adjusted with NaOH aq or HCl aq unless stated otherwise. Acetonitrile for HPLC (gradient grade) was obtained from Merck. Mammalian cell lines were purchased from the ATCC (American Type Culture Collection; Manassas, VA, USA), Sf9 cells were obtained from CLS (Eppelheim, Germany). Tissue culture flasks were procured from Sarstedt (Nümbrecht, Germany). Dulbecco's Modified Eagle's Medium - high glucose (DMEM/High;

with 4500 mg/L glucose, sodium pyruvate and sodium bicarbonate, without L-glutamine, liquid, sterile-filtered, suitable for cell culture) and L-glutamine solution (200 mM, sterile-filtered, BioXtra, suitable for cell culture) were from Sigma Aldrich. Insect-Xpress Medium was obtained from Lonza (Verviers, Belgium). Fetal calf serum (FCS) and trypsin/EDTA and were from Biochrom (Berlin, Germany). For all assays in microplate format, 96-well plates (PS, clear, F-bottom, with lid, sterile) from Greiner Bio-One (Frickenhausen, Germany) were used. The BaculoGold transfection kit was bought from BD Biosciences (San Jose, CA, USA). The Bio-Rad protein assay kit was purchased from Bio-Rad Laboratories (Munich, Germany). Syringe filters (Phenex-RC, 4 mm, 0.2  $\mu$ m) used in the chemical stability assay were from Phenomenex (Aschaffenburg, Germany).

**Stock solutions.** Topotecan and vinblastine were dissolved in 70% EtOH to give 100  $\mu$ M stock solutions. Hoechst 33342 stock solution (0.8 mM) was prepared in water and calcein-AM stock solution (100  $\mu$ M) in DMSO. The test compounds and the reference compounds fumitremorgin C, tariquidar, reversan and sulfasalazine were dissolved in DMSO at 100 times the final concentrations in the transport assays and the ATPase assay and at 1000 times the final concentrations in the chemosensitivity assay. A 1.5 mM stock solution of sulfasalazine in DMSO was prepared for stimulating ABCG2 in the inhibition mode of the ATPase Assay. Furthermore, 3 mM stock solutions of the test compounds in DMSO were prepared for the stability assay in blood plasma. If not stated otherwise, water served as solvent for other assay reagents.

**Instruments.** Fluorescence and absorbance measurements in microplates were carried out with a GENios Pro microplate reader (equipped with a Xenon arc lamp; Tecan, Grödig, Austria). Analytical HPLC of compound **59** after incubation in murine plasma was performed on a system from Agilent described above (in the chemistry part of the experimental section). The HPLC conditions were as described, yet with two alterations. The following linear gradient was applied: 0-12 min: A/B 20:80-95:5, 12-15 min: A/B 95:5. The injection volume was 100  $\mu$ L.

**Software.** All biological data were analyzed with GraphPad Prism 5 (GraphPad Software, San Diego, CA, USA).

#### 4.2.2 Cell Culture

All mammalian cells were cultured in DMEM/High supplemented with 2% (v/v) of a 200 mM L-glutamine solution and 10% (v/v) FCS at 37 °C in a water-saturated atmosphere containing 5% CO<sub>2</sub>.

**MCF-7/Topo** cells, an ABCG2-overexpressing variant of the MCF-7 cell line (ATCC<sup>®</sup> HTB-22), were obtained by passaging the MCF-7 cells with increasing amounts of topotecan in the culture medium to achieve a maximum concentration of 550 nM within a period of about 40 d; after 3 passages at the maximum concentration the treated cells expressed sufficient quantities of ABCG2 [40, 52]. They were cultured with 550 nM topotecan to maintain overexpression of the ABCG2 transporter.

**KB-V1** cells, an ABCB1-overexpressing variant of the KB cell line (ATCC<sup>®</sup> CCL-17), were obtained by passaging the KB cells with increasing amounts of vinblastine in the culture medium to achieve a maximum concentration of 330 nM within a period of about 90 d; after 3 passages at the maximum concentration the treated cells expressed sufficient quantities of ABCB1 transporter [51, 53]. They were cultured with 330 nM vinblastine to maintain overexpression of the ABCB1 transporter.

**MDCK.2-MRP1** cells were a kind gift from Prof. Dr. P. Borst from the Netherland Cancer Institute (Amsterdam, NL). They were obtained by transfecting MDCK.2 cells (ATCC<sup>®</sup> CRL-2936) with human ABCC1 [54, 55]. Due to the strong adherence of this cell line, trypsinization was performed using 2X trypsin/EDTA (0.1%/0.04%) for 30 min.

**Sf9** cells (CLS 604328) were cultured in Insect Xpress medium supplemented with 5% (v/v) FCS in 250 or 500 mL disposable Erlenmeyer flasks at 28 °C and under rotation at 150 rpm.

All cells were routinely monitored for mycoplasma contamination by PCR using the Venor<sup>®</sup>GeM mycoplasma detection kit (Minerva Biolabs, Berlin, Germany) and were negative.

#### **4.2.3 Inhibition of ABCG2: Hoechst 33342 Transport Assay [44]**

MCF-7/Topo cells were seeded into 96-well plates at a density of 20,000 cells per well (100  $\mu$ L/well) and allowed to attach to the surface of the microplates at 37 °C in a water-saturated atmosphere containing 5% CO<sub>2</sub> overnight. The next day, the culture medium was removed and the cells were incubated with loading suspension (DMEM, supplemented as described above, 8  $\mu$ M Hoechst 33342 and the test compounds at increasing concentrations; 100  $\mu$ L/well) for 2 h (37 °C, water-saturated atmosphere containing 5% CO<sub>2</sub>). FTC at a final concentration of 10  $\mu$ M served as reference compound (positive control); the vehicle DMSO (1%) served as negative control. Each concentration was measured in triplicate, positive and negative control 12-fold each. The supernatants were drained and the cells were fixed with 4% (w/w) PFA in PBS (100  $\mu$ L/well) under light protection for 20 min. Afterwards, the MCF-7/Topo cells were washed with PBS twice (250  $\mu$ L/well each time) to remove residual dye and overlaid with PBS (100  $\mu$ L/well). The relative fluorescence intensities ( $\lambda_{exc}=340$  nm,

$\lambda_{em}=485$  nm) were determined using a GENios Pro microplate reader. On each plate, the optimal gain was calculated by the determination of the fluorescence intensities in the presence of the reference substance FTC.

The data were normalized relative to the fluorescence intensity in the absence of an ABCG2 inhibitor (negative control) and the response elicited by the FTC (positive) control, which was defined as 100% inhibition of the Hoechst 33342 efflux. IC<sub>50</sub> values were calculated using four parameter sigmoidal fits. Errors were expressed as standard error of the mean (SEM).

#### **4.2.4 Inhibition of ABCB1: Calcein-AM Transport Assay [44]**

KB-V1 cells were seeded into 96-well plates at a density of 20,000 cells per well (100  $\mu$ L/well) and allowed to attach to the surface of the microplates at 37 °C in a water-saturated atmosphere containing 5% CO<sub>2</sub> overnight. The next day, the culture medium was removed and the cells were washed with loading buffer (120 mM NaCl, 5 mM KCl, 2 mM MgCl<sub>2</sub>, 1.5 mM CaCl<sub>2</sub>, 25 mM HEPES, 10 mM glucose, pH 7.4) in order to remove unspecific serum esterases. Afterwards, the cells were incubated with loading suspension (loading buffer, 5 mg/mL BSA, 1.25  $\mu$ L/mL 20% (w/w) Pluronic<sup>®</sup> F-127 in DMSO, 0.5  $\mu$ M calcein-AM and the test compounds at increasing concentrations; 100  $\mu$ L/well) for 10 min (37 °C, water-saturated atmosphere containing 5% CO<sub>2</sub>). Tariquidar at a final concentration of 10  $\mu$ M served as reference compound (positive control); the vehicle DMSO (1%) served as negative control. Each concentration was measured in triplicate, positive and negative control 12-fold each. The supernatants were drained and the cells were fixed with 4% (w/w) PFA in PBS (100  $\mu$ L/well) under light protection for 20 min. Afterwards, the KB-V1 cells were washed with PBS twice (250  $\mu$ L/well each time) to remove residual dye and overlaid with PBS (100  $\mu$ L/well). The relative fluorescence intensities ( $\lambda_{exc}=485$  nm,  $\lambda_{em}=535$  nm) were determined using a GENios Pro microplate reader. On each plate, the optimal gain was calculated by the determination of the fluorescence intensities in the presence of the reference substance tariquidar.

The data were normalized relative to the fluorescence intensity in the absence of an ABCB1 inhibitor (negative control) and the response elicited by the tariquidar (positive) control, which was defined as 100% inhibition of the calcein-AM efflux. IC<sub>50</sub> values were calculated using four parameter sigmoidal fits. Errors were expressed as standard error of the mean (SEM).

#### **4.2.5 Inhibition of ABCC1: Calcein-AM Transport Assay [41]**

MDCK.2-MRP1 cells were seeded into 96-well plates at a density of 20,000 cells per well (100  $\mu$ L/well) and allowed to attach to the surface of the microplates in a water-saturated

atmosphere containing 5% CO<sub>2</sub> at 37 °C overnight. The assay was performed and the data evaluated as described for the calcein-AM Transport Assay for analyzing ABCB1 inhibitors with two exceptions: reversan at a final concentration of 30 µM served as positive control and the incubation time was 1 h.

#### 4.2.6 ABCG2 ATPase Assay

**Generation of recombinant baculoviruses** encoding the ABCG2 protein (in the pVL1392 vector) was performed in Sf9 insect cells using the BD BaculoGold transfection kit according to the manufacturer's protocol. High-titer virus stock solutions were generated by 2-3 sequential amplifications. The supernatant fluid from the last amplification was stored at 4 °C under light protection.

**Membrane preparation.** The protocol is based on the work of Sarkadi et al. [56]. Sf9 cells with a density of 3 x 10<sup>6</sup> cells/mL (100 mL) were infected 1:500 with a high-titer ABCG2 baculovirus stock, incubated for 48 h and harvested by centrifugation at 4 °C and 500 g for 10 min. The cell pellet was re-suspended in Tris mannitol buffer (50 mM Tris, 300 mM mannitol, 0.5 mM phenylmethylsulfonyl fluoride (PMSF), pH 7; 100 mL) and centrifuged again. Then the pellet was lysed and homogenized in TMEP buffer (50 mM Tris, 50 mM mannitol, 1 mM EDTA, 10 µg/mL leupeptin, 10 µg/mL benzamidine, 0.5 mM PMSF, 2 mM DTT, pH 7; 60 mL) by a Potter Elvehjem tissue homogenizer. Undisrupted cells and cellular debris were pelleted by centrifugation at 4 °C and 500 g for 10 min and the supernatant, containing the membranes, was removed carefully. For cholesterol loading[57, 58], 2.5 mg/mL Cholesterol/RAMEB complex (cholesterol content 5.4%) was added (150 mg total) and the membranes were incubated at 4 °C for 20 min. After centrifugation at 4 °C and 100,000 g for 1 h the pellet (containing the membranes) was re-suspended in TMEP buffer (30 mL), giving a protein concentration of 2.0-3.0 mg/mL, homogenized with a Potter Elvehjem tissue homogenizer. All procedures during the membrane preparation were performed at 4 °C and aliquots (500-1000 µL) were stored at - 80 °C until use.

**Protein quantification** was performed by the method of Bradford using the Bio-Rad protein assay kit according to the manual.

**Assay procedure.** The assay was performed by analogy with the ABCB1 ATPase assay procedure described by Sarkadi et al. [56]. The ATPase activity of the ABCG2 transporter was estimated by measuring inorganic phosphate liberation. It was determined as orthovanadate-sensitive ATPase activity in the presence of inhibitors in ABCG2 Sf9 membrane preparations. The assay was carried out in the activation mode, i.e. without

stimulation of ABCG2, and in the inhibition mode, where the ABCG2 transporters in the membranes were stimulated with sulfasalazine.

Membranes containing 2.0-2.5 mg total protein were thawed on ice and pelleted by centrifugation at 4 °C and 16,200 g for 10 min. Then they were suspended in assay buffer (50 mM MOPS-Tris (100 mM MOPS, pH adjusted to 7.0 with 1.7 M Tris), 50 mM KCl, 5 mM NaN<sub>3</sub>, 2 mM EGTA, 2 mM DTT, 1 mM ouabain; 4.2 mL), mixed with 10% (w/w) CHAPS (42 µL; decreases the high basal ABCG2 ATPase activity) and homogenized using a syringe and a needle (27G). When the assay was performed in the inhibition mode, 1.5 mM sulfasalazine (10.5 µL; final conc. 3 µM) was added to the suspension to activate ABCG2. The suspension was split into 2 portions (2.0 mL each) and one portion was supplemented with orthovanadate (100 mM Na<sub>3</sub>VO<sub>4</sub>, pH 10; 50 µL; final conc. 2 mM), the other with the same amount of purified water. The two suspensions (w. and wo. orthovanadate) were transferred into a 96-well plate on ice (40 µL/well; 20-25 µg protein/well) and pre-incubated at 37 °C for 3 min.

The ATPase reaction was started by adding the reference and test compounds in assay buffer containing 20 mM ATP (10 µL/well, giving a final volume of 50 µL/well; final conc. 4 mM) with a multichannel pipette and the plate was incubated at 37 °C in a microplate shaker for 1 h. For this purpose, an ATP solution (200 mM Mg<sub>x</sub>ATP, 400 mM MgCl<sub>2</sub>, pH adjusted to 7.0 with 1.7 M Tris) was diluted 1:10 (v/v) with assay buffer and the test and reference compounds were added 5-fold concentrated. Sulfasalazine at a final concentration of 30 µM served as reference activator (positive control) in the activation mode; FTC at a final concentration of 10 µM served as reference inhibitor (positive control) in the inhibition mode; the vehicle DMSO (1% final content) served as negative control. Each concentration (w. and wo. orthovanadate) was measured in duplicate, positive and negative control in quadruplicate each.

The reaction was stopped by addition of 10% (w/w) SDS (30 µL/well); background control (phosphate stemming from the assay buffer) (w. and wo. orthovanadate) was stopped before starting the reaction with MgATP and was measured in duplicate.

Phosphate standards (0, 0.05, 0.1, 0.25, 1.5 and 2.0 mM NaH<sub>2</sub>PO<sub>4</sub> in assay buffer; 50 µL/well; each concentration measured in duplicate) were included on each plate for calibration.

The amount of phosphate was determined by adding a colorimetric reagent (1 part of reagent A (35 mM ammonium molybdate, 15 mM zinc acetate) mixed with 4 parts of reagent B (5% (w/w) ascorbic acid, pH 5.0; freshly prepared); 200 µL/well) and by incubating

at 37 °C for further 20 min. The absorbance (820 nm) as a parameter proportional to the phosphate amount was measured, using a GENios Pro microplate reader.

Data obtained under the treatment with orthovanadate were subtracted from the data without orthovanadate to obtain phosphate liberation resulting from ABCG2 activity. The ensuing data were normalized relative to the absorbance in the absence of an ABCG2 activator/inhibitor (negative control) and the response elicited by the sulfasalazine (positive) control, which was defined as 100% ATPase activity in the activation mode, or the response elicited by the FTC (positive) control, which was defined as 0% ATPase activity in the inhibition mode of the assay, where the membranes were activated with sulfasalazine. IC<sub>50</sub> values were calculated using four parameter sigmoidal fits. Errors were expressed as standard error of the mean (SEM).

#### **4.2.7 Size-Exclusion Chromatography-Based Thermostability Assay (SEC-TS)**

**Expression and purification of human ABCG2** was performed as described in our previous report [39].

**Assay procedure.** The assay was carried out as described in our previous study [39]. In short: Detergent-purified ABCG2 was incubated with or without the test compound at a concentration of 10 μM for 10 min at room temperature. Samples were aliquoted (100 μL each) and heated at one temperature, ranging from 30-75 °C, for 10 min in a Bio-Rad Thermocycler. Then the samples were cooled on ice, centrifuged at 4 °C and 100,000 g for 20 min and subjected to HP-SEC, using a TSKgel G3000SWxl column (Tosoh Biosciences) as stationary phase and a detection wavelength of 280 nm.  $T_m$  values were calculated using four parameter sigmoidal fits. Errors were expressed as standard deviation (SD) of the best fit values.

#### **4.2.8 Chemosensitivity Assay [59]**

MCF-7/Topo cells were seeded into 96-well plates at a density of 1500 cells per well (100 μL/well) and allowed to attach to the surface of the microplates in a water-saturated atmosphere containing 5% CO<sub>2</sub> at 37 °C overnight. The next day, fresh medium containing the test compounds at 2-fold final concentrations was added (100 μL/well; giving a final volume of 200 μL/well). On each plate, vinblastine at a final concentration of 300 nM served as reference cytostatic (positive control); the vehicle DMSO (0.1%) served as negative control to monitor cell growth in the absence of a drug. Each concentration was measured 8-fold, positive and negative control 16-fold each. Growth of the cells was stopped after different

periods of time by removal of medium and fixation with 2% (v/v) glutardialdehyde in PBS. All the plates were stored at 4 °C until the end of the experiment and afterwards stained with 0.02% crystal violet (100 µL/well) for 20 min. Excess dye was removed by rinsing the plates with water three times. Crystal violet bound by the fixed cells was re-dissolved in 70% EtOH (180 µL/well) while shaking the microplates for 2-3 h. The absorbance (580 nm) as a parameter proportional to the cell mass was measured using a GENios Pro microplate reader. Cytotoxic effects were expressed as corrected T/C-values according to

$$T / C_{corr} [\%] = \frac{T - C_0}{C - C_0} \cdot 100$$

where T is the mean absorbance of the treated cells, C the mean absorbance of the growth controls and  $C_0$  the mean absorbance of the cells at the time of compound addition ( $t_0$ ). When the absorbance of treated cells T was lower than at the beginning of the experiment ( $C_0$ ), the extent of cell killing was calculated as cytocidal effect according to

$$Cytocidal \ effect \ [\%] = \frac{T - C_0}{C_0} \cdot 100$$

#### 4.2.9 Chemical Stability Assay (in Blood Plasma) [41]

The blood from NMRI (nu/nu) mice was collected by cardiac puncture in deep anesthesia using heparinized syringes. To remove cellular components, the samples were immediately centrifuged at 4 °C and 4500 g for 7 min and the supernatant was carefully removed. The plasma samples were stored at - 80 °C.

Stock solutions of the test compounds (3 mM in DMSO) were diluted 1:50 with murine plasma giving a concentration of 60 µM. The samples were vortexed shortly and incubated at 37 °C. After different periods of time, aliquots were taken and deproteinated by adding two parts of ice-cold MeCN, vortexing and storing at 4 °C for 30 min. Samples were centrifuged at 4 °C and 14,000 g for 5 min and the supernatants were filtered with syringe filters, diluted 1:1 with MeCN and stored at - 80 °C until analyzed. They were thawed at room temperature and analyzed with HPLC.

## Ancillary Content

Supporting information related to this article can be found.

Preparation of the intermediate and target compounds and corresponding analytical data.  $^1\text{H}$  NMR and  $^{13}\text{C}$  NMR spectra of the target compounds. RP-HPLC analysis (purity control) of key target compounds.

## Author Information

### Corresponding Authors

\* E-mail: frau.antonio@ur.de. Phone: (+49)941-943-2925. Fax: (+49)941-943-4820.

\* E-mail: burkhard.koenig@ur.de. Phone: (+49)941-943-4575. Fax: (+49)941-943-1717.

### Author Contributions

F.A. wrote the manuscript with supervision from G.B. and with input from all co-authors. The junior authors performed the experiments and analyzed the data with supervision from B.K., K.P.L., A.B and G.B. (Synthesis: M.B., S.A.S., F.A. Transport Assays: S.B., F.A., M.S., S.A.S. ATPase Assays: M.S. Thermostability Assays: S.M.J. and I.M. Chemosensitivity Assays: F.A. Chemical Stability Assays: F.A.)

### Note

# A.B. deceased in July 18, 2017.

### Competing Interest

The authors declare no competing financial interest.

## Acknowledgements

This work was supported by the Swiss National Science Foundation program NCCR TransCure. The authors thank Maria Beer-Krön and Lydia Schneider for their excellent technical assistance and Marlies Antoni for her insightful linguistic advice.

## Abbreviations

ABC, ATP-binding cassette transporter; ABCB1, ATP-binding cassette transporter, subfamily B, member 1; ABCC1, ATP-binding cassette transporter, subfamily C, member 1; ABCG2, ATP-binding cassette transporter, subfamily G, member 2; ADP, adenosine diphosphate; ATP, adenosine triphosphate; BBB, blood-brain barrier; BCRP, breast cancer resistance protein; CHAPS, 3-((3-cholamidopropyl)dimethylammonio)-1-propanesulfonate; cryo-EM, cryogenic electron microscopy; CuAAC, copper-catalyzed azide-alkyne cycloaddition; DCM, dichloromethane; DIPEA, N,N-diisopropylethylamine; DMEM, Dulbecco's modified Eagle's medium; DMF, dimethylformamide; DMSO, dimethylsulfoxide; DTT, dithiothreitol; EC<sub>50</sub>, concentration of compound required to give 50% maximal effect on activity; EDTA, ethylenediaminetetraacetic acid; FCS, fetal calf serum; FTC, fumitremorgin C; HBTU,

hexafluorophosphate benzotriazole tetramethyl uronium; HPLC, high pressure liquid chromatography; IC<sub>50</sub>, concentration of inhibitor required to give 50% inhibition of activity; IR, infrared; MDR, multidrug resistance; MRP1, multidrug resistance associated protein 1; NMR, nuclear magnetic resonance; NMRI, Naval Medical Research Institute; PBS, phosphate buffered saline; PCR, polymerase chain reaction; Pd/C, palladium on activated charcoal; PEG, polyethylene glycol; P-gp, permeability glycoprotein; PMSF, phenylmethylsulfonyl fluoride; RAMEB, randomly methylated  $\beta$ -cyclodextrins; SDS, sodium dodecyl sulfate; SEC-TS, size-exclusion chromatography-based thermostability assay; SEM, standard error of the mean; TBAF, tetra-n-butylammonium fluoride; TBTA, tris((1-benzyl-4-triazolyl)methyl)amine; TFA, trifluoroacetic acid; THF, tetrahydrofuran; TLC, thin layer chromatography; TMS, trimethylsilyl; Tris, tris(hydroxymethyl)aminomethane.

## References

- [1] Y.N. Chen, L.A. Mickley, A.M. Schwartz, E.M. Acton, J. Hwang, A.T. Fojo, Characterization of adriamycin-resistant human breast cancer cells which display overexpression of a novel resistance-related membrane protein, *J. Biol. Chem.*, 265 (1990) 10073-10080.
- [2] L.A. Doyle, W. Yang, L.V. Abruzzo, T. Krogmann, Y. Gao, A.K. Rishi, D.D. Ross, A multidrug resistance transporter from human MCF-7 breast cancer cells, *Proc. Natl. Acad. Sci. U. S. A.*, 96 (1999) 2569.
- [3] F. Staud, P. Pavek, Breast cancer resistance protein (BCRP/ABCG2), *Int. J. Biochem. Cell Biol.*, 37 (2005) 720-725.
- [4] M.M. Gottesman, T. Fojo, S.E. Bates, Multidrug resistance in cancer: role of ATP-dependent transporters, *Nat. Rev. Cancer*, 2 (2002) 48-58.
- [5] G.D. Eytan, Mechanism of multidrug resistance in relation to passive membrane permeation, *Biomed. Pharmacother.*, 59 (2005) 90-97.
- [6] H.R. Mellor, R. Callaghan, Resistance to Chemotherapy in Cancer: A Complex and Integrated Cellular Response, *Pharmacology*, 81 (2008) 275-300.
- [7] B.C. Baguley, Multiple Drug Resistance Mechanisms in Cancer, *Mol. Biotechnol.*, 46 (2010) 308-316.
- [8] D.J. Begley, ABC transporters and the blood-brain barrier, *Curr. Pharm. Des.*, 10 (2004) 1295-1312.
- [9] C. Ghosh, V. Puvenna, J. Gonzalez-Martinez, D. Janigro, N. Marchi, Blood-brain barrier P450 enzymes and multidrug transporters in drug resistance: a synergistic role in neurological diseases, *Curr. Drug Metab.*, 12 (2011) 742-749.
- [10] A. Mahringer, G. Fricker, ABC transporters at the blood-brain barrier, *Expert Opin. Drug Metab. Toxicol.*, 12 (2016) 499-508.
- [11] M. Hubensack, C. Mueller, P. Hoecherl, S. Fellner, T. Spruss, G. Bernhardt, A. Buschauer, Effect of the ABCB1 modulators elacridar and tariquidar on the distribution of paclitaxel in nude mice, *J. Cancer Res. Clin. Oncol.*, 134 (2008) 597-607.
- [12] M.H. Hasanabady, F. Kalalinia, ABCG2 inhibition as a therapeutic approach for overcoming multidrug resistance in cancer, *J. Biosci.*, 41 (2016) 313-324.

- [13] J.W. Ricci, D.M. Lovato, V. Severns, L.A. Sklar, R.S. Larson, Novel ABCG2 Antagonists Reverse Topotecan-Mediated Chemotherapeutic Resistance in Ovarian Carcinoma Xenografts, *Mol. Cancer Ther.*, 15 (2016) 2853-2862.
- [14] M.C. de Gooijer, N.A. de Vries, T. Buckle, L.C.M. Buil, J.H. Beijnen, W. Boogerd, O. van Tellingen, Improved Brain Penetration and Antitumor Efficacy of Temozolomide by Inhibition of ABCB1 and ABCG2, *Neoplasia*, 20 (2018) 710-720.
- [15] A. Karbownik, K. Sobańska, W. Płotek, T. Grabowski, A. Klupczynska, S. Plewa, E. Grześkowiak, E. Szalek, The influence of the coadministration of the p-glycoprotein modulator elacridar on the pharmacokinetics of lapatinib and its distribution in the brain and cerebrospinal fluid, *Invest. New Drugs*, (2019).
- [16] M. Bauer, R. Karch, B. Wulkersdorfer, C. Philippe, L. Nics, E.-M. Klebermass, M. Weber, S. Poschner, H. Haslacher, W. Jaeger, N. Tournier, W. Wadsak, M. Hacker, M. Zeitlinger, O. Langer, A proof-of-concept study to inhibit ABCG2- and ABCB1- mediated efflux transport at the human blood-brain barrier, *J. Nucl. Med.*, 60 (2019) 486-491.
- [17] S. Dauchy, F. Dutheil, R.J. Weaver, F. Chassoux, C. Daumas-Duport, P.-O. Couraud, J.-M. Scherrmann, I. De Waziers, X. Decleves, ABC transporters, cytochromes P450 and their main transcription factors: expression at the human blood-brain barrier, *J. Neurochem.*, 107 (2008) 1518-1528.
- [18] R. Shawahna, Y. Uchida, X. Decleves, S. Ohtsuki, S. Yousif, S. Dauchy, A. Jacob, F. Chassoux, C. Daumas-Duport, P.-O. Couraud, T. Terasaki, J.-M. Scherrmann, Transcriptomic and Quantitative Proteomic Analysis of Transporters and Drug Metabolizing Enzymes in Freshly Isolated Human Brain Microvessels, *Mol. Pharmaceutics*, 8 (2011) 1332-1341.
- [19] F. Hyafil, C. Vergely, P. Du Vignaud, T. Grand-Perret, In vitro and in vivo reversal of multidrug resistance by GF120918, an acridonecarboxamide derivative, *Cancer Res.*, 53 (1993) 4595-4602.
- [20] M. de Bruin, K. Miyake, T. Litman, R. Robey, S.E. Bates, Reversal of resistance by GF120918 in cell lines expressing the ABC half-transporter, MXR, *Cancer Lett.*, 146 (1999) 117-126.
- [21] M. Roe, A. Folkes, P. Ashworth, J. Brumwell, L. Chima, S. Hunjan, I. Pretswell, W. Dangerfield, H. Ryder, P. Charlton, Reversal of P-glycoprotein mediated multidrug resistance by novel anthranilamide derivatives, *Bioorg. Med. Chem. Lett.*, 9 (1999) 595-600.
- [22] R.W. Robey, K. Steadman, O. Polgar, K. Morisaki, M. Blayney, P. Mistry, S.E. Bates, Pheophorbide a Is a Specific Probe for ABCG2 Function and Inhibition, *Cancer Res.*, 64 (2004) 1242-1246.
- [23] S.K. Rabindran, H. He, M. Singh, E. Brown, K.I. Collins, T. Annable, L.M. Greenberger, Reversal of a novel multidrug resistance mechanism in human colon carcinoma cells by fumitremorgin C, *Cancer Res.*, 58 (1998) 5850-5858.
- [24] J.D. Allen, A. Van Loevezijn, J.M. Lakhai, M. Van der Valk, O. Van Tellingen, G. Reid, J.H.M. Schellens, G.-J. Koomen, A.H. Schinkel, Potent and specific inhibition of the breast cancer resistance protein multidrug transporter in vitro and in mouse intestine by a novel analogue of fumitremorgin C, *Mol. Cancer Ther.*, 1 (2002) 417-425.
- [25] L.D. Weidner, S.S. Zoghbi, S. Lu, S. Shukla, S.V. Ambudkar, V.W. Pike, J. Mulder, M.M. Gottesman, R.B. Innis, M.D. Hall, The inhibitor Ko143 is not specific for ABCG2, *J. Pharmacol. Exp. Ther.*, 354 (2015) 384-393.
- [26] S.A.L. Zander, J.H. Beijnen, O. van Tellingen, Sensitive method for plasma and tumor Ko143 quantification using reversed-phase high-performance liquid chromatography and fluorescence detection, *J. Chromatogr. B: Anal. Technol. Biomed. Life Sci.*, 913-914 (2013) 129-136.
- [27] K. Liu, J. Zhu, Y. Huang, C. Li, J. Lu, M. Sachar, S. Li, X. Ma, Metabolism of Ko143, an ABCG2 inhibitor, *Drug Metab. Pharmacokinet.*, 32 (2017) 193-200.

- [28] A. Spindler, K. Stefan, M. Wiese, Synthesis and Investigation of Tetrahydro- $\beta$ -carboline Derivatives as Inhibitors of the Breast Cancer Resistance Protein (ABCG2), *J. Med. Chem.*, 59 (2016) 6121-6135.
- [29] W. Chearwae, S. Shukla, P. Limtrakul, S.V. Ambudkar, Modulation of the function of the multidrug resistance-linked ATP-binding cassette transporter ABCG2 by the cancer chemopreventive agent curcumin, *Mol. Cancer Ther.*, 5 (2006) 1995-2006.
- [30] E. Nicolle, J. Boccard, D. Guilet, M.-G. Dijoux-Franca, F. Zelefac, S. Macalou, J. Grosselin, J. Schmidt, P.-A. Carrupt, A. Di Pietro, A. Boumendjel, Breast cancer resistance protein (BCRP/ABCG2): New inhibitors and QSAR studies by a 3D linear solvation energy approach, *Eur. J. Pharm. Sci.*, 38 (2009) 39-46.
- [31] K. Takada, N. Imamura, K.R. Gustafson, C.J. Henrich, Synthesis and structure-activity relationship of botryllamides that block the ABCG2 multidrug transporter, *Bioorg. Med. Chem. Lett.*, 20 (2010) 1330-1333.
- [32] J. Gallus, K. Juvale, M. Wiese, Characterization of 3-methoxy flavones for their interaction with ABCG2 as suggested by ATPase activity, *Biochim. Biophys. Acta, Biomembr.*, 1838 (2014) 2929-2938.
- [33] N. Sjostedt, K. Holvikari, P. Tammela, H. Kidron, Inhibition of Breast Cancer Resistance Protein and Multidrug Resistance Associated Protein 2 by Natural Compounds and Their Derivatives, *Mol. Pharmaceutics*, 14 (2017) 135-146.
- [34] K. Silbermann, C.P. Shah, N.U. Sahu, K. Juvale, S.M. Stefan, P.S. Kharkar, M. Wiese, Novel chalcone and flavone derivatives as selective and dual inhibitors of the transport proteins ABCB1 and ABCG2, *Eur. J. Med. Chem.*, 164 (2019) 193-213.
- [35] G. Valdameri, E. Genoux-Bastide, B. Peres, C. Gauthier, J. Guitton, R. Terreux, S.M.B. Winnischofer, M.E.M. Rocha, A. Boumendjel, A. Di Pietro, Substituted Chromones as Highly Potent Nontoxic Inhibitors, Specific for the Breast Cancer Resistance Protein, *J. Med. Chem.*, 55 (2012) 966-970.
- [36] R. Yamazaki, H. Hatano, T. Yaegashi, Y. Igarashi, O. Yoshida, Y. Sugimoto, Preparation of 3-[4-(4-hydroxypiperidin-1-yl)thiophen-2-yl]-2-phenylacrylonitrile 2-(cyclic amino)acetyl esters as breast cancer resistance protein (ABCG2) inhibitors, in, *Kabushiki Kaisha Yakult Honsha, Japan* . 2009, pp. 42pp.
- [37] R. Yamazaki, Y. Nishiyama, T. Furuta, H. Hatano, Y. Igarashi, N. Asakawa, H. Kodaira, H. Takahashi, R. Aiyama, T. Matsuzaki, N. Yagi, Y. Sugimoto, Novel Acrylonitrile Derivatives, YHO-13177 and YHO-13351, Reverse BCRP/ABCG2-Mediated Drug Resistance In Vitro and In Vivo, *Mol. Cancer Ther.*, 10 (2011) 1252-1263.
- [38] N.M.I. Taylor, I. Manolaridis, S.M. Jackson, J. Kowal, H. Stahlberg, K.P. Locher, Structure of the human multidrug transporter ABCG2, *Nature*, 546 (2017) 504-509.
- [39] S.M. Jackson, I. Manolaridis, J. Kowal, M. Zechner, N.M.I. Taylor, M. Bause, S. Bauer, R. Bartholomaeus, G. Bernhardt, B. Koenig, A. Buschauer, H. Stahlberg, K.-H. Altmann, K.P. Locher, Structural basis of small-molecule inhibition of human multidrug transporter ABCG2, *Nat. Struct. Mol. Biol.*, 25 (2018) 333-340.
- [40] M. Kühnle, M. Egger, C. Müller, A. Mahringer, G. Bernhardt, G. Fricker, B. König, A. Buschauer, Potent and Selective Inhibitors of Breast Cancer Resistance Protein (ABCG2) Derived from the p-Glycoprotein (ABCB1) Modulator Tariquidar, *J. Med. Chem.*, 52 (2009) 1190-1197.
- [41] S. Bauer, C. Ochoa-Puentes, Q. Sun, M. Bause, G. Bernhardt, B. Koenig, A. Buschauer, Quinoline Carboxamide-Type ABCG2 Modulators: Indole and Quinoline Moieties as Anilide Replacements, *ChemMedChem*, 8 (2013) 1773-1778.
- [42] L. Liang, D. Astruc, The copper(I)-catalyzed alkyne-azide cycloaddition (CuAAC) "click" reaction and its applications. An overview, *Coord. Chem. Rev.*, 255 (2011) 2933-2945.

- [43] T.R. Chan, R. Hilgraf, K.B. Sharpless, V.V. Fokin, Polytriazoles as Copper(I)-Stabilizing Ligands in Catalysis, *Org. Lett.*, 6 (2004) 2853-2855.
- [44] C.O. Puentes, P. Höcherl, M. Kühnle, S. Bauer, K. Bürger, G. Bernhardt, A. Buschauer, B. König, Solid phase synthesis of tariquidar-related modulators of ABC transporters preferring breast cancer resistance protein (ABCG2), *Bioorg. Med. Chem. Lett.*, 21 (2011) 3654-3657.
- [45] C. Ochoa-Puentes, S. Bauer, M. Kühnle, G. Bernhardt, A. Buschauer, B. König, Benzanilide–Biphenyl Replacement: A Bioisosteric Approach to Quinoline Carboxamide-Type ABCG2 Modulators, *ACS Med. Chem. Lett.*, 4 (2013) 393-396.
- [46] J.E. Obrique-Balboa, Q. Sun, G. Bernhardt, B. König, A. Buschauer, Flavonoid derivatives as selective ABCC1 modulators: Synthesis and functional characterization, *Eur. J. Med. Chem.*, 109 (2016) 124-133.
- [47] S. Kraege, K. Stefan, K. Juvalé, T. Ross, T. Willmes, M. Wiese, The combination of quinazoline and chalcone moieties leads to novel potent heterodimeric modulators of breast cancer resistance protein (BCRP/ABCG2), *Eur. J. Med. Chem.*, 117 (2016) 212-229.
- [48] T. Litman, T.E. Druley, W.D. Stein, S.E. Bates, From MDR to MXR: new understanding of multidrug resistance systems, their properties and clinical significance, *Cell. Mol. Life Sci.*, 58 (2001) 931-959.
- [49] T. Reya, S.J. Morrison, M.F. Clarke, I.L. Weissman, Stem cells, cancer, and cancer stem cells, *Nature*, 414 (2001) 105-111.
- [50] H. Itatani, J.C. Bailar, Homogenous catalysis in the reactions of olefinic substances. V. Hydrogenation of soybean oil methyl ester with triphenylphosphine and triphenylarsine palladium catalysts, *J. Am. Oil Chem. Soc.*, 44 (1967) 147-151.
- [51] M. Hubensack, Approaches to Overcome the Blood-Brain Barrier in the Chemotherapy of Primary and Secondary Brain Tumors: Modulation of P-glycoprotein 170 and Targeting of the Transferrin Receptor, Dissertation, University of Regensburg, <https://epub.uni-regensburg.de/10297/>, 2005.
- [52] C.-H. Yang, E. Schneider, M.-L. Kuo, E.L. Volk, E. Rocchi, Y.-C. Chen, BCRP/MXR/ABCP expression in topotecan-resistant human breast carcinoma cells, *Biochem. Pharmacol.*, 60 (2000) 831-837.
- [53] K. Kohno, J. Kikuchi, S. Sato, H. Takano, Y. Saburi, K. Asoh, M. Kuwano, Vincristine-resistant human cancer KB cell line and increased expression of multidrug-resistance gene, *Jpn. J. Cancer Res.*, 79 (1988) 1238-1246.
- [54] R. Evers, M. Kool, L. van Deemter, H. Janssen, J. Calafat, L.C. Oomen, C.C. Paulusma, R.P. Oude Elferink, F. Baas, A.H. Schinkel, P. Borst, Drug export activity of the human canalicular multispecific organic anion transporter in polarized kidney MDCK cells expressing cMOAT (MRP2) cDNA, *J. Clin. Invest.*, 101 (1998) 1310-1319.
- [55] E. Bakos, R. Evers, G. Szakacs, G.E. Tusnady, E. Welker, K. Szabo, M. De Haas, L. Van Deemter, P. Borst, A. Varadi, B. Sarkadi, Functional multidrug resistance protein (MRP1) lacking the N-terminal transmembrane domain, *J. Biol. Chem.*, 273 (1998) 32167-32175.
- [56] B. Sarkadi, E.M. Price, R.C. Boucher, U.A. Germann, G.A. Scarborough, Expression of the human multidrug resistance cDNA in insect cells generates a high activity drug-stimulated membrane ATPase, *J. Biol. Chem.*, 267 (1992) 4854-4858.
- [57] A. Telbisz, M. Mueller, C. Ozvegy-Laczka, L. Homolya, L. Szenté, A. Varadi, B. Sarkadi, Membrane cholesterol selectively modulates the activity of the human ABCG2 multidrug transporter, *Biochim. Biophys. Acta, Biomembr.*, 1768 (2007) 2698-2713.
- [58] A. Pal, D. Mehn, E. Molnar, S. Gedey, P. Meszaros, T. Nagy, H. Glavinas, T. Janaky, O. von Richter, G. Bathori, L. Szenté, P. Krajcsi, Cholesterol potentiates ABCG2 activity in a heterologous expression system: improved in vitro model to study function of human ABCG2, *J. Pharmacol. Exp. Ther.*, 321 (2007) 1085-1094.

[59] G. Bernhardt, H. Reile, H. Birnböck, T. Spruß, H. Schönenberger, Standardized kinetic microassay to quantify differential chemosensitivity on the basis of proliferative activity, *J. Cancer Res. Clin. Oncol.*, 118 (1992) 35-43.

Journal Pre-proof

## Highlights

### **Tariquidar-Related Triazoles as Potent, Selective and Stable Inhibitors of ABCG2 (BCRP)**

Frauke Antoni<sup>a,\*</sup>, Manuel Bause<sup>b</sup>, Matthias Scholler<sup>a</sup>, Stefanie Bauer<sup>a</sup>, Simone A. Stark<sup>b</sup>, Scott M. Jackson<sup>c</sup>, Ioannis Manolaridis<sup>c</sup>, Kaspar P. Locher<sup>c</sup>, Burkhard König<sup>b,\*</sup>, Armin Buschauer<sup>a,#</sup>, Günther Bernhardt<sup>a</sup>

<sup>a</sup> *Institute of Pharmacy, University of Regensburg, D-93040 Regensburg, Germany*

<sup>b</sup> *Institute of Organic Chemistry, University of Regensburg, D-93040 Regensburg, Germany*

<sup>c</sup> *Institute of Molecular Biology and Biophysics, ETH Zürich, CH-8093 Zürich, Switzerland*

- Tariquidar-related ABCG2 inhibitors were synthesized and functionally characterized
- The compounds are among the most potent ABCG2 inhibitors described so far
- High selectivity for ABCG2 could be achieved
- Reduction of the ABCG2 ATPase activity was identified as one inhibition mechanism
- Stability in blood plasma was proven

**Declaration of interests**

The authors declare that they have no known competing financial interests or personal relationships that could have appeared to influence the work reported in this paper.

The authors declare the following financial interests/personal relationships which may be considered as potential competing interests: